Journal of Medicinal Chemistry

Subscriber access provided by TRINITY COLL

Article

Hydroxybiphenylamide GroEL/ES inhibitors are potent antibacterials against planktonic and biofilm forms of *Staphylococcus aureus*

Trent Kunkle, Sanofar Abdeen, Nilshad Salim, Anne-Marie Ray, Mckayla Stevens, Andrew J Ambrose, Jose Victorino, Yangshin Park, Quyen Q. Hoang, Eli Chapman, and Steven M Johnson

J. Med. Chem., **Just Accepted Manuscript** • DOI: 10.1021/acs.jmedchem.8b01293 • Publication Date (Web): 04 Nov 2018

Downloaded from http://pubs.acs.org on November 7, 2018

Just Accepted

"Just Accepted" manuscripts have been peer-reviewed and accepted for publication. They are posted online prior to technical editing, formatting for publication and author proofing. The American Chemical Society provides "Just Accepted" as a service to the research community to expedite the dissemination of scientific material as soon as possible after acceptance. "Just Accepted" manuscripts appear in full in PDF format accompanied by an HTML abstract. "Just Accepted" manuscripts have been fully peer reviewed, but should not be considered the official version of record. They are citable by the Digital Object Identifier (DOI®). "Just Accepted" is an optional service offered to authors. Therefore, the "Just Accepted" Web site may not include all articles that will be published in the journal. After a manuscript is technically edited and formatted, it will be removed from the "Just Accepted" Web site and published as an ASAP article. Note that technical editing may introduce minor changes to the manuscript text and/or graphics which could affect content, and all legal disclaimers and ethical guidelines that apply to the journal pertain. ACS cannot be held responsible for errors or consequences arising from the use of information contained in these "Just Accepted" manuscripts.

ACS Publications

is published by the American Chemical Society. 1155 Sixteenth Street N.W., Washington, DC 20036

Published by American Chemical Society. Copyright © American Chemical Society. However, no copyright claim is made to original U.S. Government works, or works produced by employees of any Commonwealth realm Crown government in the course of their duties.

Hydroxybiphenylamide GroEL/ES inhibitors are potent antibacterials against planktonic and biofilm forms of *Staphylococcus aureus*.

AUTHOR NAMES

Trent Kunkle,[a,1] Sanofar Abdeen,[a,1] Nilshad Salim,[a] Anne-Marie Ray,[a] Mckayla Stevens,[a] Andrew J. Ambrose,[b] José Victorino,[a] Yangshin Park,[a,c,d] Quyen Q. Hoang,[a,c,d] Eli Chapman,[b] and Steven M. Johnson[a,*]

[1] Co-first author

AUTHOR ADDRESSES

[a] Indiana University School of Medicine, Department of Biochemistry and Molecular Biology, 635 Barnhill Dr., Indianapolis, IN 46202

[b] The University of Arizona, College of Pharmacy, Department of Pharmacology and Toxicology, 1703 E. Mabel St., PO Box 210207, Tucson, AZ 85721

[c] Stark Neurosciences Research Institute, Indiana University School of Medicine. 320 W. 15th Street, Suite 414, Indianapolis, IN 46202

[d] Department of Neurology, Indiana University School of Medicine. 635 Barnhill Drive, Indianapolis, IN 46202

KEYWORDS.

GroEL, GroES, HSP60, HSP10, molecular chaperone, chaperonin, proteostasis, small molecule inhibitors, *ESKAPE* pathogens, MRSA, antibiotics.

ABSTRACT

We recently reported the identification of a GroEL/ES inhibitor (**1**: *N*-(4-(benzo[*d*]thiazol-2-ylthio)-3-chlorophenyl)-3,5-dibromo-2-hydroxybenzamide) that exhibited *in vitro* antibacterial effects against *Staphylococcus aureus* comparable to vancomycin, an antibiotic of last resort. To follow-up, we have synthesized 43 compound **1** analogs to determine the most effective functional groups of the scaffold for inhibiting GroEL/ES and killing bacteria. Our results identified that the benzothiazole and hydroxyl groups are important for inhibiting GroEL/ES-mediated folding functions, with the hydroxyl essential for antibacterial effects. Several analogs exhibited >50-fold selectivity indices between antibacterial efficacy and cytotoxicity to human liver and kidney cells in cell culture. We found that MRSA were not able to easily generate acute resistance to lead inhibitors in a gain-of-resistance assay, and that lead inhibitors were able to permeate through established *S. aureus* biofilms and maintain their bactericidal effects.

INTRODUCTION:

In 2013, the Centers for Disease Control and Prevention (CDC) released a report highlighting the dangers posed by multi-drug resistant bacteria, in particular a group of six that have been termed the ***ESKAPE*** pathogens: ***E****nterococcus faecium* (Gram-positive), ***S****taphylococcus aureus* (Gram-positive), ***K****lebsiella pneumoniae* (Gram-negative), ***A****cinetobacter baumannii* (Gram-negative), ***P****seudomonas aeruginosa* (Gram-negative), and the ***E****nterobacter* species (Gram-negative).[1] The report estimated that these bacteria infect over two-million people in the U.S. annually, leading to ~23,000 deaths. Of the *ESKAPE* pathogens, methicillin-resistant strains of *S. aureus* (MRSA) were found to be the deadliest, causing ~80,000 infections and ~11,000 deaths annually. Unfortunately, the development of new antibiotics over the past four decades has continually declined, and continuing research programs tend to focus on re-derivatizing already known antibacterial classes.[2-4] In addition, many bacteria are intrinsically able to evade antibiotic effects by forming biofilms, which are often hallmarks of chronic infections.[5] While vancomycin is effective at treating planktonic *S. aureus*, it is not able to penetrate and kill bacteria within biofilms.[6, 7] Thus, to circumvent these resistance mechanisms, there is an urgent need for antibacterials that function through new mechanisms of action and previously unexploited pathways.

While disrupting protein homeostasis has proven to be an effective antibacterial strategy in the context of inhibiting the transcriptional and translational machineries, perturbing protein folding pathways has gone largely unexplored.[3] To facilitate newly synthesized polypeptides folding into their active/native structural conformations, cells utilize a class of accessory proteins termed molecular chaperones, also known as Heat Shock Proteins (HSPs).[8] When molecular chaperone functions are compromised, non-native polypeptides could misfold and aggregate,

which is detrimental to cell viability.[9-12] Thus, targeting molecular chaperones with small molecule inhibitors should be an effective strategy for killing bacteria that is unique from the mechanisms of current antibiotics. While significant efforts have been made to target HSP70 and HSP90 chaperones for developing anti-cancer agents, researchers are now beginning to explore these chaperones as antibiotic targets.[13-20] However, targeting HSP60 chaperonin systems, called GroEL chaperonins in bacteria, has gone largely unexplored. GroEL is a homo-tetradecameric protein complex that consists of two, seven-membered rings that stack back-to-back with each other. GroEL functions to refold nascent polypeptides through a mechanism unique from other molecular chaperones. To facilitate the folding of substrate polypeptides, GroEL requires binding of ATP and a co-chaperone, called GroES. GroES binding to the GroEL apical domains encapsulates the substrate polypeptides within the central cavity of GroEL, where they can attempt to fold while being sequestered from the outside environment. Details of the GroEL/ES-mediated folding cycle have been extensively investigated and reported elsewhere.[21-27]

Since the GroEL/ES system is essential for bacterial viability under all conditions, we hypothesize that blocking its functions with small molecule inhibitors should be an effective antibacterial strategy.[28, 29] A caveat to this strategy is that human HSP60 is moderately conserved with the bacterial homologs (48% identity with the prototypical GroEL chaperonin from *Escherichia coli*), which raises the question of potential off-target effects against human cells. However, HSP60 is localized within the mitochondrial matrix of human cells, which is highly impermeable to small molecules. Thus, even if compounds can inhibit HSP60 *in vitro*, they may not reach and inhibit it in the mitochondrial matrix, permitting selective targeting of bacteria over human cells.

In a previous study, we performed high-throughput screening and identified 235 inhibitors of the GroEL/ES folding cycle.[30] In a follow-up study evaluating a subset of these GroEL/ES inhibitors for their antibacterial effects against the *ESKAPE* pathogens, we identified compound **1** (**Figure 1A**) as a hit candidate for further antibacterial development.[31] In particular, compound **1** exhibited bactericidal effects against *S. aureus* that were comparable to vancomycin (i.e. sub-μM EC_{50}). While compound **1** exhibited low-to-moderate cytotoxicity against human liver (THLE-3) and kidney (HEK 293) cell lines, it still had >50-fold selectivity indices for killing *S. aureus* bacteria. Intriguingly, compound **1** has been reported to have anthelmintic activity against *Trichocephalus muris*, and two anthelmintic drugs used to treat parasitic infections in livestock, closantel and rafoxanide (**Figure 1B**), bear striking resemblances to the compound **1** scaffold.[32, 33] In addition, Cheng *et al.* reported similar analogs that exhibited anti-MRSA activities, although the reported structure-activity relationships (SAR) suggested that their antibacterial effects were not entirely through targeting transglycosylase activity.[34] Thus, there is a high probability that targeting the GroEL/ES chaperonin system could be contributing significantly to its antibacterial effects, which warrants further investigation.

While compound **1** itself is a promising GroEL/ES inhibitor to take forward as an anti-bacterial candidate, there is room for further optimization before proceeding into a proof-of-principle anti-bacterial efficacy models in animals (e.g. mice systemically infected with *S. aureus*). As a first step in our optimization strategy, rather than adding various substituents and substructures to the scaffold as is often done in drug development, we chose an opposite approach and employed a molecular deconstruction strategy where we systematically removed the various substituents and substructures (**R^1-R^5 – Figure 1A**) to evaluate their contributions to inhibitor potency and selectivity. Thus, we synthesized a library of 43 analogs that contained all

the different ± combinations of the **R^1-R^5** groups. We then tested them in a series of assays to achieve three primary objectives: 1) determine which groups are crucial to inhibit GroEL/ES and HSP60/10 folding function *in vitro*; 2) identify groups that expand the therapeutic window further between antibacterial efficacy and human cell cytotoxicity; and 3) determine if inhibitors are effective against bacteria in biofilms, and whether or not bacteria will be able to generate acute resistance to this molecular class. Results from these assays would then allow us to identify the smallest effective inhibitor analog that maintains potency against bacteria while reducing cytotoxicity to human cells. Knowing this information would then allow us to build upon this base scaffold in a more rational approach to improve the pharmacological properties of this antibacterial series.

RESULTS AND DISCUSSION

Evaluating the effectiveness of compound 1 analogs for inhibiting the GroEL/ES-mediated folding cycle.

As a first step in this study, we synthesized analogs **1-44** using well-established chemistry as outlined in **Scheme 1**. A nucleophilic aromatic substitution reaction between 2-mercaptobenzothiazole and 3,4-dichloronitrobenzene was employed to give the nitro-intermediate **45** (containing the chloro-group in the **R^2** position), which was subsequently reduced to the amine **46** using tin powder in a 10% mixture of HCl in AcOH.[32, 35-38] The intermediate amine **47**, lacking the chloro-group at the **R^2** position, was synthesized in one step by a nucleophilic aromatic substitution reaction between 2-chlorobenzothiazole and aminothiophenol.[39] Compounds **17-44** were prepared by reacting the respective aryl-acid chlorides (where commercially available) with amines **46** or **47** with pyridine in anhydrous

dicloromethane.[36, 37] If only the respective aryl-carboxylic acids were commercially available, we either converted them to their acid chloride counter-parts by reacting with thionyl chloride, or coupled the acids directly to the amines using amide coupling procedures with DDC, DMAP, and pyridine, or EDC, HOBt•H_2O, and TEA in dichloromethane.[37] The methoxy-bearing analogs (**29-44**) were then further de-methylated to analogs **1-16** using BBr_3 in anhydrous dichloromethane.[36-38, 40] Detailed synthetic protocols and compound characterizations (e.g. ^{1}H-NMR, MS, and RP-HPLC) are presented in the Experimental Section and Supporting Information. We also purchased the two highly related anthelmintic drugs used in veterinary medicine, closantel and rafoxanide, to determine whether they would also inhibit the GroEL/ES chaperonin system. While their mode of action is reported to involve uncoupling of the proton gradient of oxidative phosphorylation, which drives ATP production in the mitochondria of parasites, it is possible that targeting GroEL/ES or HSP60/10 chaperonin systems could be contributing to their antibiotic properties.[41, 42]

After generating the compound library, we next employed a series of well-established biochemical assays to evaluate compound inhibitory effects against the GroEL/ES chaperonin system. As in previous studies, we used *E. coli* GroEL/ES as the surrogate chaperonin system for refolding of the reporter enzymes malate dehydrogenase (MDH) and rhodanese (Rho).[30, 31, 40] Briefly, binary complexes are formed between GroEL and denatured MDH or Rho, which are then refolded to their native states upon addition of ATP and the GroES co-chaperonin. Enzymatic activities of refolded native MDH or Rho act as coupled reporters of GroEL/ES refolding functions since in the presence of chaperonin inhibitors, no functional reporter enzymes are generated. Inhibition IC_{50} results for testing of compounds in these two refolding assays are compiled in **Table 1**, and visually presented in the correlation plot in **Figure 2A**. The

log-transformations of IC_{50} results and standard deviations are presented in **Table S1** in the Supporting Information. As seen in **Figure 2A**, there is a strong correlation between compounds inhibiting in the GroEL/ES-dMDH and dRho refolding assays (Spearman correlation coefficient comparing log(IC_{50}) values in each assay is 0.9663, $p < 0.0001$), suggesting they are acting on-target against the chaperonin system. As we do not know where the binding sites are for this series of inhibitors, precise structure-function interpretation of the results remains elusive. In general, though, the $\mathbf{R^1}$-benzothiazole coupled with the $\mathbf{R^3}$-hydroxyl are required for potent inhibition. Halogenation at the $\mathbf{R^2}$-position (Cl) and $\mathbf{R^4}$/$\mathbf{R^5}$ positions (Br) further increases inhibitor potency, likely through a combination of increased hydrophobic interactions of the halides themselves, coupled with the electron-withdrawing capability of the bromines lowering the pK_a of the salicylate hydroxyl, which could enhance polar interactions within the binding sites. Perhaps not surprisingly, we found that closantel and rafoxanide were, indeed, potent GroEL/ES inhibitors; thus, an intriguing question to address in future studies will be how much does targeting chaperonin systems contribute to the anthelmintic effects of these two veterinary antibiotics?

To further support on-target effects, we evaluated inhibitors against the native MDH and Rho enzymes to identify false-positives that simply inhibit the reporter reactions of the coupled refolding assays (detailed procedures are presented in the Supporting Information). While some compounds were found to inhibit native MDH (e.g. **1**, **5**, closantel, and to lesser extents, **9**, **13**, and rafoxanide), none of the analogs were found to inhibit native Rho enzymatic activity (**Table 1** and **Figure 2B**). While these results further support that inhibitors are targeting the chaperonin-mediated folding cycle, they also indicate that selectivity issues may be a liability that future studies would need to address. Hearteningly, though, a few analogs (e.g. compound

2, **3**, **6**, and **7**) are moderate to potent inhibitors in the GroEL/ES-mediated refolding assays yet remained inactive against the reporter enzymes, suggesting selectivity concerns are not insurmountable.

Determining the antibacterial effects of compounds against the *ESKAPE* pathogens.

We next evaluated compounds for antibacterial efficacy against the *ESKAPE* pathogens in liquid media culture as per previously reported procedures.[38] Inhibition EC_{50} results for testing of compounds in these bacterial proliferation assays are shown in **Table 2**. In general, this series of analogs was ineffective against the Gram-negative bacteria (*K. pneumonia*, *A. baumannii*, *P. aeruginosa*, and *E. cloacae*), likely owing to drug efflux and/or impermeability to the lipopolysaccharide (LPS) outer membranes of Gram-negative bacteria.[31] However, with regards to *A. baumannii*, notable exceptions are compounds **2** and **6**, which exhibit EC_{50} values of 2.9 and 12 μM, respectively. This suggests that drug efflux and LPS impermeability issues may not be insurmountable with further inhibitor optimization. As previously observed with compound **1**, several analogs retained antibacterial efficacy against the Gram-positive bacteria, *E. faecium* and *S. aureus*, although they were strikingly more effective against *S. aureus*. The presence of the hydroxyl at the $\mathbf{R^3}$ position appears to be integral for potent inhibition of *S. aureus* bacteria, almost regardless of substituents and substructures at the other positions. However, it is noted that incorporation of the benzothiazole substructure at the $\mathbf{R^1}$ position leads to the most potent inhibitors (and generally required to inhibit *E. faecium*), which may support on-target effects since these analogs are all equipotent against the MRSA strain that we evaluated

compounds against (ATCC #BAA-44, HPV107 designation, isolated from a hospital in Lisbon, Portugal).

When comparing the EC_{50} results of this series of compounds against *E. faecium* bacteria with the IC_{50} values obtained in the GroEL/ES-dMDH refolding assay (**Figure 3A**), we note an almost linear correlation (Spearman correlation coefficient comparing $\log(I/EC_{50})$ values in each assay is 0.9628, $p < 0.0001$), which may indicate on-target effects against GroEL/ES driving antibacterial activity. When performing the same comparison with MRSA bacteria (**Figure 3B**), although a trend is evident between antibacterial efficacy and GroEL/ES inhibition MRSA (Spearman correlation coefficient comparing $\log(I/EC_{50})$ values in each assay is 0.8042, $p < 0.0001$), several compounds that are not GroEL/ES inhibitors still remain effective against bacteria (e.g. **10-16**). This finding could be a result of *S. aureus* GroEL/ES functioning differently than the *E. coli* GroEL/ES chaperonin system, which we use as a surrogate in these studies; however, we cannot rule out potential off-target effects, especially since we know that some analogs could inhibit MDH and also potentially be targeting transglycosylase as reported by Cheng *et al.*[34] Further studies are warranted to determine how *E. faecium* and *S. aureus* GroEL/ES function compared to *E. coli* GroEL/ES, and to identify the specific mechanisms of action of these inhibitors in both *E. faecium* and *S. aureus* bacteria.

While some GroEL/ES inhibitors can target human HSP60/10 *in vitro*, many display moderate to low cytotoxicity to human cells.

Knowing which compounds were effective GroEL/ES inhibitors with antibacterial properties, we next evaluated whether they would 1) inhibit human HSP60/10, and 2) exhibit cytotoxicity to two cell lines that we typically employ for cell viability testing *in vitro*: THLE-3

liver cells and HEK 293 kidney cells. These assays were performed as previously reported, with detailed protocols presented in the Supporting Information.[31, 38, 40] Briefly, the HSP60/10-dMDH folding assay was conducted analogously to the GroEL/ES-dMDH folding assay so IC_{50} results could be directly compared. The human cell cytotoxicity assays used Alamar Blue reagents to measure the viability of liver and kidney cells that had been incubated with test compounds over a 48 h time period. Biochemical inhibition (IC_{50}) and cell viability (cytotoxicity; CC_{50}) results for these assays are presented in **Table 3**.

While some analogs selectively inhibit *E. coli* GroEL/ES over human HSP60/10 (e.g. **3**, **4**, **7**, and **8**), IC_{50} values between the GroEL/ES-dMDH and HSP60/10-dMDH folding assays were nearly the same for most analogs (**Figure 4A** - Spearman correlation coefficient comparing $\log(IC_{50})$ values in each assay is 0.8351, $p < 0.0001$). We note, though, that comparison of these results is convoluted by the fact that some of these analogs also inhibit native MDH, and thus could be false positives in the HSP60/10-dMDH folding assay owing to simply inhibiting the MDH reporter reaction. While HSP60/10 inhibition could potentially be teased out by employing rhodanese as the denatured reporter enzyme as we do in the case of the GroEL/ES-dRho refolding assay, in our experience, the equivalent HSP60/10-dRho refolding is not as robust, potentially owing to the lower stability of human HSP60 compared to *E. coli* GroEL.

When comparing the biochemical and cell-based results, there does not appear to be a noticeable correlation between HSP60/10-dMDH refolding assay IC_{50} values and liver and kidney cell viability assay CC_{50} values (**Figure 4B** - (Spearman correlation coefficient values are 0.4791 ($p < 0.0008$) and 0.3286 ($p < 0.0258$) when comparing HSP60/10-dMDH refolding assay $\log(IC_{50})$ values with liver and kidney cell viability $\log(CC_{50})$ values, respectively). Interestingly, compounds that bear the $\mathbf{R^1}$ benzothiazole and $\mathbf{R^3}$ hydroxyl substructures (**1**-**8**) are

generally less cytotoxic against the HEK 293 cells than their counterparts without the **R**[1] benzothiazole (**9-16**), and also less cytotoxic to the THLE-3 liver cells. Since inclusion of these two substructures generally afforded more potent chaperonin inhibitors, the differences between these results may suggest that compound cytotoxicities are predominantly a result of off-target effects and not from targeting HSP60/10 itself. This would not be surprising since some analogs are also able to inhibit native MDH (e.g. **1**, **5**, **9**, **13**, closantel, and rafoxanide). When comparing EC_{50} values of compounds inhibiting the proliferation of susceptible and methicillin-resistant *S. aureus* with cell viability CC_{50} values against the human liver and kidney cells (**Figure 4C**), we note that many analogs exhibit >50-fold selectivity indices. Considering we have only been looking at the effects that removing substituents and substructures have on the potency and selectivity of this series of analogs, these are exciting initial results to move forward from in future med-chem efforts where we begin to append and optimize the various substituents and substructures of this scaffold.

MRSA cannot readily generate acute resistance to lead analogs.

After identifying which compounds selectively inhibited the GroEL chaperonin system and killed bacteria, we next evaluated whether bacteria could quickly develop resistance to lead candidate inhibitors. This was a concern we encountered with another series of GroEL/ES inhibitors we have been studying, represented by the bis-sulfonamido compound "**28R**" shown in **Figure 5**.[38] For this experiment, we adapted a liquid culture resistance assay from the previously established procedures of Kim *et al.*, and used our MRSA strain as the test bacteria (a detailed procedure is presented in the Supporting Information).[38, 43] Briefly, test compounds were incubated in dilution series with MRSA for 24 h and EC_{50} values were determined. The

first well exhibiting OD_{600} readings >0.2 were then sub-cultured for another 24 h with test compound again in dilution series. Serial passage in this manner was conducted for a total of 12 days, and each day EC_{50} values for the test compounds were determined: inhibitors to which MRSA could rapidly generate resistance would exhibit increasing EC_{50} results over each successive passage. Rapid resistance was observed for the previously reported bis-sulfonamide compound, **28R**, but was found to be reversible and likely owing to increased inhibitor efflux.[38] We evaluated two of our lead GroEL inhibitors, **1** and **11**, along with vancomycin, and found that all three exhibited exemplary antibiotic efficacy to which this MRSA strain was not able to easily generate resistance.

Compound 1 is bactericidal to *S. aureus* within established biofilms

While we found that *S. aureus* is not able to easily generate resistance to compounds **1** and **11**, what remained to be seen was whether this series of inhibitors would be effective at preventing bacteria from establishing biofilms and killing bacteria within already established biofilms. Establishing biofilms is another effective mechanism by which *S. aureus* can evade the effects of many current antibiotics, including vancomycin. To gauge the efficacy of lead inhibitors at preventing *S. aureus* from forming biofilms, we employed an assay similar to the liquid culture assay we used to determine inhibition of bacterial proliferation, with a few modifications (detailed procedures presented in the Experimental section). Briefly, test compounds (**1**, **2**, **5**, **8**, **11**, and vancomycin) were incubated with *S. aureus* bacteria in media supplemented with 0.5% glucose (to support biofilm formation) for 24 h at 37°C. After 24 h, the supernatant was removed, the wells were gently washed, and the biofilm that had formed on the well surfaces were stained with crystal-violet and quantified by UV-Vis spectroscopy. We found

that all of the compound **1** analogs tested, and vancomycin, were able to prevent *S. aureus* from forming biofilms with EC_{50} values nearly equipotent to antibacterial EC_{50}s we determined against planktonic bacterial growth. Representative dose-response curves for compound **1** and vancomycin tested in these assays are presented in **Figure 6**, with a tabulation of test compound EC_{50} results presented in **Table 4**. The high correlation of these results was not entirely surprising as compound **1** and vancomycin are bactericidal against *S. aureus*, and thus dead bacteria would not be able to form biofilms.[31]

Next, we evaluated whether or not compounds would be bactericidal to *S. aureus* that were within already established biofilms. In this assay, we first grew *S. aureus* bacteria for 24 h in the absence of test compounds so that they could establish biofilms in the wells. After 24 h, the cultures were removed, the wells were washed gently, and fresh media was added along with test compounds or vancomycin. The cultures were incubated in the presence of test compounds for another 24 h, then the wells were gently washed again to remove compounds and any planktonic bacteria that had emerged. Fresh media was then added and the cultures were incubated for another 24 h to allow any viable bacteria remaining in the biofilms to emerge and grow planktonically again. While there were 5-15-fold shifts in EC_{50} values for the compound **1** analogs killing planktonic *vs.* biofilm bacteria (**Figure 6** and **Table 4**), these are still exciting results considering vancomycin was completely ineffective against biofilm bacteria (EC_{50} >100 μM), and especially since this class of GroEL/ES inhibitors has yet to be fully optimized. Thus, this scaffold shows considerable promise to take forward for further development as an antibacterial candidate.

CONCLUSIONS

In the present study, we developed a series of analogs of the previously identified hit GroEL inhibitor, compound **1**, and employed a molecular deconstruction strategy to systematically evaluate the contributions that the $\mathbf{R^1}$ to $\mathbf{R^5}$ substituents and substructures make towards selectively inhibiting the GroEL/ES chaperonin system and killing bacteria. We found that the benzothiazole $\mathbf{R^1}$ group and hydroxyl $\mathbf{R^2}$ substituent were integral to inhibiting GroEL/ES *in vitro*, but that the hydroxyl was the key determinant for being able to potently inhibit *S. aureus* proliferation. While trends are noted between IC_{50} values from the GroEL/ES-dMDH refolding assay and the *E. faecium* and *S. aureus* proliferation assays, further experiments are warranted to conclusively determine whether or not inhibitors are on-target in bacteria. While some inhibitors were equipotent in the human HSP60/10-dMDH refolding assay, several exhibited only moderate to low cytotoxicity to liver and kidney cells. Importantly, compounds **1** and **11** did not encounter acute resistance through a 12-day serial passage in MRSA, generally maintaining efficacy <1 μM. Furthermore, compound **1** analogs were effective at killing *S. aureus* bacteria within established biofilms, whereas vancomycin was ineffective. These exemplary results support future med-chem derivatization efforts to optimize the *in vitro* and *in vivo* pharmacological properties of this class of GroEL/ES inhibitors for antibacterial development.

EXPERIMENTAL

General Synthetic Methods.

Unless otherwise stated, all chemicals were purchased from commercial suppliers and used without further purification. Reaction progress was monitored by thin-layer chromatography on silica gel 60 F254 coated glass plates (EM Sciences). Flash chromatography

was performed using a Biotage Isolera One flash chromatography system with elution through Biotage KP-Sil Zip or Snap silica gel columns for normal-phase separations (hexanes:EtOAc gradients) or Snap KP-C18-HS columns for reverse-phase separations (H_2O:MeOH gradients). Reverse-phase high-performance liquid chromatography (RP-HPLC) was performed using a Waters 1525 binary pump, 2489 tunable UV/Vis detector (254 and 280 nm detection), and 2707 autosampler. For preparatory HPLC purification, samples were chromatographically separated using a Waters XSelect CSH C18 OBD prep column (part number 186005422, 130 Å pore size, 5 μm particle size, 19x150 mm), eluting with a H_2O:CH_3CN gradient solvent system. Linear gradients were run from either 100:0, 80:20, or 60:40 A:B to 0:100 A:B (A = 95:5 H_2O:CH_3CN, 0.05% TFA; B = 5:95 H_2O:CH_3CN, 0.05% TFA. Products from normal-phase separations were concentrated directly, and reverse-phase separations were concentrated, diluted with H_2O, frozen, and lyophilized. For primary compound purity analyses (HPLC-1), samples were chromatographically separated using a Waters XSelect CSH C18 column (part number 186005282, 130 Å pore size, 5 μm particle size, 3.0x150 mm), eluting with the above H_2O:CH_3CN gradient solvent systems. For secondary purity analyses (HPLC-2) of final test compounds, samples were chromatographically separated using a Waters XBridge C18 column (either part number 186003027, 130 Å pore size, 3.5 μm particle size, 3.0x100 mm, or part number 186003132, 130 Å pore size, 5.0 μm particle size, 3.0x100 mm), eluting with a H_2O:MeOH gradient solvent system. Linear gradients were run from either 100:0, 80:20, 60:40, or 20:80 A:B to 0:100 A:B (A = 95:5 H_2O:MeOH, 0.05% TFA; B = 5:95 H_2O:MeOH, 0.05% TFA). Test compounds were found to be >95% pure from both RP-HPLC analyses. Mass spectrometry data were collected using either an Agilent analytical LC-MS at the IU Chemical Genomics Core Facility (CGCF), or a Thermo-Finnigan LTQ LC-MS in-lab. ^{1}H-NMR spectra

were recorded on a Bruker 300 MHz spectrometer at the CGCF. Chemical shifts are reported in parts per million and calibrated to the d_6-DMSO solvent peaks at 2.50 ppm. Synthesis and characterization of intermediates **45-49** are presented below. General amide coupling and methoxy deprotection steps are presented as follows using compounds **29** and **1** as representative examples. Specific synthetic procedures and compound characterizations are presented in the Supporting Information for the remaining analogs.

45: 2-((2-Chloro-4-nitrophenyl)thio)benzo[*d*]thiazole. 2-Mercaptobenzothiazole (11.9 g, 71.1 mmol), 3,4-dichloronitrobenzene (11.8 g, 61.5 mmol), and potassium carbonate (11.7 g, 84.7 mmol) were stirred together in DMF (60 mL) at R.T. overnight, then at 80°C for 4 h. The reaction was then diluted with water and the precipitate was filtered, rinsed with water, and dried to afford **45** as a yellow powder (19.5 g, 98% yield). ^{1}H-NMR (300 MHz, d_6-DMSO) δ 8.51 (d, J = 2.4 Hz, 1H), 8.23 (dd, J = 8.7, 2.5 Hz, 1H), 8.10 (d, J = 7.8 Hz, 1H), 8.07-8.13 (m, 1H), 7.91 (d, J = 8.7 Hz, 1H), 7.44-7.59 (m, 2H); MS (ESI) $C_{13}H_8ClN_2O_2S_2$ $[MH]^+$ *m/z* expected = 323.0, observed = 323.1; HPLC-1 = 98%.

46: 4-(Benzo[*d*]thiazol-2-ylthio)-3-chloroaniline. Tin powder (5.64 g, 47.5 mmol) was added slowly to a stirring mixture of **45** in a 1:10 mixture of HCl:AcOH (15 mL). The reaction was allowed to stir at R.T. for 2 days, then diluted with EtOAc and H_2O, neutralized with $NaHCO_3$, and filtered. The filtrate was extracted with EtOAc and the organics dried over Na_2SO_4, filtered, and concentrated. The crude product was then chromatographed over silica (hexanes:EtOAc gradient) and concentrated. The residue was diluted in a 4:1 mixture of hexanes:DCM and the precipitate was filtered and dried to afford **46** as a yellow powder (3.73 g, 81% yield). ^{1}H-NMR

(300 MHz, d_6-DMSO) δ 7.87-7.96 (m, 1H), 7.80 (d, J = 8.1 Hz, 1H), 7.53 (d, J = 8.5 Hz, 1H), 7.43 (td, J = 7.7, 1.3 Hz, 1H), 7.26-7.34 (m, 1H), 6.87 (d, J = 2.4 Hz, 1H), 6.64 (dd, J = 8.5, 2.4 Hz, 1H), 6.18 (s, 2H); MS (ESI) $C_{13}H_{10}ClN_2S_2$ $[MH]^+$ *m/z* expected = 293.0, observed = 293.0; HPLC-1 = 98%.

47: 4-(Benzo[*d*]thiazol-2-ylthio)aniline. 2-Chlorobenzothiazole (2.00 g, 11.8 mmol), 4-aminothiophenol (1.70 g, 13.6 mmol), and potassium carbonate (3.24 g, 23.4 mmol) were stirred together in EtOH (15 mL) for 18 h. The reaction was then diluted with water and the precipitate was filtered, rinsed with water, and collected. Flash chromatographic purification (hexanes:EtOAc gradient) afforded **47** as an off-white solid (2.71 g, 89% yield). ^{1}H-NMR (300 MHz, d_6-DMSO) δ 7.85-7.91 (m, 1H), 7.78 (d, J = 7.7 Hz, 1H), 7.37-7.45 (m, 3H), 7.25-7.34 (m, 1H), 6.66-6.73 (m, 2H), 5.84 (s, 1H); MS (ESI) $C_{13}H_{11}N_2S_2$ $[MH]^+$ *m/z* expected = 259.0, observed = 259.0; HPLC-1 = >99%.

48: 3,5-Dibromo-2-methoxybenzoic acid. Iodomethane (6.30 mL, 101 mmol), 3,5-dibromosalicylic acid (10.0 g, 33.7 mmol), and K_2CO_3 (14.0 g, 101 mmol) were stirred at R.T. overnight, then at 80°C for 4 h. The reaction was diluted into water and extracted into DCM. The organics were dried over Na_2SO_4, filtered, and concentrated. The intermediate ester was then stirred overnight with LiOH•H_2O (5.70 g, 136 mmol) in a 3:1:1 mixture of THF:MeOH:H_2O (35 mL). The reaction was diluted with water and acidified with HCl. The precipitate was filtered, washed with water, and dried to afford **48** as a white solid (9.85 g, 94% yield). ^{1}H-NMR (300 MHz, d_6-DMSO) δ 13.56 (br s, 1H), 8.09 (d, J = 2.5 Hz, 1H), 7.83 (d, J =

2.5 Hz, 1H), 3.81 (s, 3H); MS (ESI) $C_8H_5Br_2O_3$ [M-H]$^-$ *m/z* expected = 308.9, observed = 309.1; HPLC-1 = >99%.

49: 5-Bromo-2-methoxybenzoic acid. 5-Bromosalicylic acid (10.0 g, 46.1 mmol), iodomethane (8.60 mL, 138 mmol), and K_2CO_3 (19.0 g, 137 mmol) were stirred at R.T. overnight, then at 80°C for 4 h. The reaction was diluted into water and the precipitate was filtered, rinsed with water, and dried. The intermediate ester was then stirred overnight with LiOH•H_2O (7.70 g, 184 mmol) in a 3:1:1 mixture of THF:MeOH:H_2O (45 mL). The reaction was diluted with water and acidified with HCl. The precipitate was filtered, washed with water, and dried to afford **49** as a white solid (8.70 g, 82% yield). ^{1}H-NMR (300 MHz, d_6-DMSO) δ 12.98 (br s, 1H), 7.72 (d, *J* = 2.6 Hz, 1H), 7.66 (dd, *J* = 8.8, 2.6 Hz, 1H), 7.10 (d, *J* = 8.9 Hz, 1H), 3.81 (s, 3H); MS (ESI) $C_8H_6BrO_3$ [M-H]$^-$ *m/z* expected = 229.0, observed = 229.0; HPLC-1 = 98%.

General procedure for the amide coupling step using analog 29 as a representative example: *N*-(4-(Benzo[*d*]thiazol-2-ylthio)-3-chlorophenyl)-3,5-dibromo-2-methoxybenzamide. Compound **48** (225 mg, 0.726 mmol) was stirred in $SOCl_2$ (2 mL) at 60°C for 1 h, then was concentrated. Anhydrous DCM (5 mL), compound **46** (148 mg, 0.505 mmol), and pyridine (62.0 µL, 0.760 mmol) were added and the reaction was stirred at R.T. for 18 h (under Ar). Flash chromatographic purification (hexanes:EtOAc gradient) afforded **29** as a yellow solid (58.6 mg, 20% yield). ^{1}H-NMR (300 MHz, d_6-DMSO) δ 11.00 (s, 1H), 8.21 (d, *J* = 2.1 Hz, 1H), 8.10 (d, *J* = 2.3 Hz, 1H), 7.97 (t, *J* = 8.3 Hz, 2H), 7.82-7.87 (m, 2H), 7.78 (dd, *J* = 8.6, 2.2 Hz, 1H), 7.47 (td, *J* = 7.7, 1.3 Hz, 1H), 7.32-7.38 (m, 1H), 3.84 (s, 3H); MS (ESI)

$C_{21}H_{12}Br_2ClN_2O_2S_2$ [M-H]$^-$ *m/z* expected = 580.8, observed = 580.7; HPLC-1 = >99%; HPLC-2 = >99%.

General procedure for the methoxy deprotection step to give hydroxylated compounds using analog 1 as a representative example: *N*-(4-(Benzo[*d*]thiazol-2-ylthio)-3-chlorophenyl)-3,5-dibromo-2-hydroxybenzamide. To a stirring mixture of **29** (51.0 mg, 0.0872 mmol) in anhydrous DCM (5 mL) was added BBr_3 (0.26 mL of 1 M in DCM, 0.26 mmol). The reaction was allowed to stir at R.T. (under Ar) for 18 h and then quenched with MeOH. Flash chromatographic purification (hexanes:EtOAc gradient) afforded **1** as an off-white solid (34.4 mg, 69% yield). ^{1}H-NMR (300 MHz, d_6-DMSO) δ 11.14 (br s, 1H), 8.19 (dd, J = 6.2, 2.2 Hz, 2H), 7.94-8.05 (m, 3H), 7.82-7.89 (m, 2H), 7.47 (td, J = 7.7, 1.3 Hz, 1H), 7.33-7.40 (m, 1H); MS (ESI) $C_{20}H_{10}Br_2ClN_2O_2S_2$ [M-H]$^-$ *m/z* expected = 566.8, observed = 566.6; HPLC-1 = 99%; HPLC-2 = 98%.

Protein Expression and purification.

E. coli GroEL and GroES, and human HSP60 and HSP10, were expressed and purified as previously reported.[30, 31, 38, 40, 44] Detailed protocols for these protein purifications are presented in the Supporting Information.

Control compounds for assays.

For all of the biochemical assays (GroEL/ES and HSP60/10-mediated dMDH and dRho refolding assays, and native MDH and Rho enzymatic activity counter-screens), DMSO was used as negative control, and a panel of our previously discovered and reported chaperonin

inhibitors were used as positive controls: e.g. compound **1** herein; compounds **9** and **18** from Johnson *et. al* 2014 and Abdeen *et. al* 2016[30, 31]; suramin and compound **2h-*p*** from Abdeen *et. al* 2016[40]; and compounds **20R**, **20L**, and **28R** from Abdeen *et. al* 2018.[38] For the bacterial proliferation assays, control compounds included the aforementioned panel of previously reported chaperonin inhibitors as well as vancomycin, daptomycin, ampicillin, and rifampicin. For the human cell viability assays, control compounds include the aforementioned compounds as well as other protein homeostasis inhibitors, such as bortezomib (proteasome inhibitor); VER-155008 (HSP70 inhibitor); and ganetespib and 17-DMAG (HSP90 inhibitors).

Evaluation of compounds in GroEL/ES and HSP60/10-mediated dMDH and dRho refolding assays.

All compounds were evaluated for inhibiting *E. coli* GroEL/ES and human HSP60/10-mediated refolding of the denatured MDH and denatured Rho reporter enzymes as per previously reported procedures.[30, 31, 38, 40] Detailed protocols for these assays are presented in the Supporting Information.

Counter-screening compounds for inhibition of native MDH and Rho enzymatic activity.

All compounds were counter-screened for inhibiting the enzymatic activity of the native MDH and native Rho reporter enzymes as per previously reported procedures.[30, 31, 38, 40] Detailed protocols for the assays are presented in the Supporting Information.

Cell information for compound evaluation.

The *ESKAPE* bacteria were purchased from the American Type Culture Collection (ATCC): *E. faecium* (Orla-Jensen) Schleifer and Kilpper-Balz strain NCTC 7171 (ATCC 19434); *S. aureus* subsp. *aureus* Rosenbach strain Seattle 1945 (ATCC 25923); Multi-drug resistant *S. aureus* (MRSA) subsp. *aureus* Rosenbach strain HPV107 (ATCC BAA-44); *K. pneumonia*, subsp. *pneumoniae* (Schroeter) Trevisan strain NCTC 9633 (ATCC 13883); *A. baumannii* Bouvet and Grimont strain 2208 (ATCC 19606); *P. aeruginosa* (Schroeter) Migula strain NCTC 10332 (ATCC 10145); *E. cloacae*, subsp. *cloacae* (Jordan) Hormaeche and Edwards strain CDC 442-68 (ATCC 13047). Human THLE-3 liver cells (ATCC CRL-11233) and HEK 293 kidney cells (ATCC CRL-1573) were used for the cell viability assays.

Evaluation of compounds for inhibition of bacterial cell proliferation.

All compounds were evaluated for inhibiting the proliferation of each of the *ESKAPE* bacteria as per previously reported procedures.[38] Detailed protocols for bacterial growth assays are presented in the Supporting Information.

Evaluation of compound effects on HEK 293 and THLE-3 cell viability.

All compounds were evaluated for cytotoxicities to THLE-3 liver and HEK 293 kidney cells using Alamar Blue-based viability assays as per previously reported procedures.[31, 38, 40] Detailed protocols for these assays are presented in the Supporting Information.

Evaluation of MRSA resistance generation against lead inhibitors.

To identify potential resistance toward compounds **1** and **11**, a liquid culture, 12-day serial passage assay was employed as per previously reported procedures, and using the ATCC

BAA-44 MRSA strain.[38, 43, 45] A detailed protocol for this assay is presented in the Supporting Information.

***S. aureus* Biofilm Prevention Assay.**

The biofilm prevention assay was carried out with *S. aureus* Rosenbach (ATCC 25923) using a quantitative crystal violet-based adherence assay on 96-well plates as described previously by Kwasny *et al*.[46] *S. aureus* (ATCC 25923) bacteria were streaked onto a Tryptic Soy Broth (TSB) agar plate and grown overnight at 37°C. A fresh aliquot of TSB media was inoculated with a single bacterial colony and the cultures were grown overnight at 37°C with shaking (250 rpm). The overnight culture was then sub-cultured (1:5 dilution) into a fresh aliquot of TSB media supplemented to a final concentration of 0.5% glucose and grown at 37°C for 1 h with shaking, then diluted into fresh TSB media supplemented with 0.5% glucose to achieve a final OD_{600} reading of 0.01. Aliquots of the diluted culture (100 μL) were dispensed to 96 well polystyrene plates along with addition of 1 μL test compounds in DMSO. The inhibitor concentration range during the assay was 100 μM to 46 nM (3-fold dilution series). A second set of baseline control plates were prepared analogously, but without any bacteria added, to correct for possible compound absorbance and/or precipitation. Plates were sealed with "Breathe Easy" oxygen permeable membranes (Diversified Biotech) and left to incubate at 37°C without shaking (stagnant assay) until the biofilm was formed. After 24 h, the planktonic cultures were removed and the plates were washed gently 2-3 times with 200 μl of water. Next, the plates were air dried and the adherent biofilms were stained with 150 μL of crystal violet solution (2.3% crystal violet in 20% Ethanol, Sigma Aldrich #HT90132) for 15 minutes at R.T. The unbound crystal violet stain was removed, then plates were gently washed again with running water and air dried for 10

min. Quantitative assessment of biofilm formation was obtained by adding 100 μL of developer solution (4:1:5 mixture of MeOH:AcOH:H_2O) per well. Well absorbance was then read at 595 nm using a Molecular Devices SpectraMax Plus384 microplate reader. EC_{50} values for the test compounds were obtained by plotting the $A_{595\ nm}$ results in GraphPad Prism 6 and analyzing by non-linear regression using the log(inhibitor) vs. response (variable slope) equation. Results presented represent the averages of EC_{50} values obtained from at least triplicate experiments.

***S. aureus* Biofilm Penetration and Bactericidal Activity Assay.**

The biofilm penetration and bactericidal activity assay was carried out with *S. aureus* Rosenbach (ATCC 25923) as described previously by Kwasny *et al*.[46] *S. aureus* bacteria were streaked onto a Tryptic Soy Broth (TSB) agar plate and grown overnight at 37°C. A fresh aliquot of TSB media was inoculated with a single bacterial colony and the cultures were grown overnight at 37°C with shaking (250 rpm). The overnight culture was then sub-cultured (1:5 dilution) into a fresh aliquot of TSB media supplemented with 0.5% glucose and grown at 37°C for 1 h with shaking, then diluted into fresh TSB media supplemented with 0.5% glucose to achieve a final OD_{600} reading of 0.01. Aliquots of the diluted culture (100 μL) were dispensed to 96 well polystyrene plates without any compounds added. A second set of control plates were prepared analogously, but without any bacteria added. Plates were sealed with "Breathe Easy" oxygen permeable membranes (Diversified Biotech) and left to incubate at 37°C without shaking (stagnant assay) until biofilm was formed. After 24 h, the planktonic cultures (or media blanks in the control plates) were removed and the plates were washed gently 3 times with 200 μL of sterile phosphate buffered saline (PBS). Then, 100 μL aliquots of fresh TSB media were dispensed to the plates along with addition of 1 μL of test compounds in DMSO. The inhibitor

concentration range during the assay was 100 μM to 46 nM (3-fold dilution series). The plates were sealed with "Breathe Easy" membranes and incubated at 37°C without shaking to allow compounds to penetrate and kill bacteria in the biofilms. After 24 h, the cultures were removed and plates were washed again gently 3 times with 200 μL of sterile PBS. The remaining bacteria in the biofilms were allowed to recover by adding 100 μL of fresh TSB media per well and incubating for 24 h at 37°C. At the end of this final incubation, bacterial growth was monitored by measuring the $OD_{600\ nm}$ using a Molecular Devices SpectraMax Plus384 microplate reader. EC_{50} values for the test compounds were obtained by plotting the $OD_{600\ nm}$ results in GraphPad Prism 6 and analyzing by non-linear regression using the log(inhibitor) vs. response (variable slope) equation. Results presented represent the averages of EC_{50} values obtained from at least triplicate experiments.

Calculation of IC_{50} / EC_{50} / CC_{50} values and statistical considerations.

All IC_{50} / EC_{50} / CC_{50} results reported are averages of values determined from individual dose-response curves in assay replicates as follows: 1) Individual I/E/CC_{50} values from assay replicates were first log-transformed and the average log(I/E/CC_{50}) values and standard deviations (SD) calculated; 2) Replicate log(I/E/CC_{50}) values were evaluated for outliers using the ROUT method in GraphPad Prism 6 (Q of 10%); and 3) Average I/E/CC_{50} values were then back-calculated from the average log(I/E/CC_{50}) values. To compare log(I/E/CC_{50}) values between different assays, two-tailed Spearman correlation analyses were performed using GraphPad Prism 6 (95% confidence level). For compounds where log(I/E/CC_{50}) values were greater than the maximum compound concentrations tested (i.e. >2.0, or >100 μM), results were represented as 0.1 log units higher than the maximum concentrations tested (i.e. 2.1, or 126 μM),

so as not to overly bias comparisons because of the unavailability of definitive values for these inactive compounds.

Corresponding Author

* E-mail: johnstm@iu.edu, Phone: 317-274-2458, Fax: 317-274-4686.

ACKNOWLEDGMENTS

Research reported in this publication was supported by the National Institute of General Medical Sciences (NIGMS) of the National Institutes of Health (NIH) under Award Number R01GM120350. QQH and YP additionally acknowledge support by NIH grants 5R01GM111639 and 5R01GM115844. The content is solely the responsibility of the authors and does not necessarily represent the official views of the NIH. This work was also supported in part by startup funds from the IU School of Medicine (SMJ) and the University of Arizona (EC). The human HSP60 expression plasmid (lacking the 26 amino acid *N*-terminal mitochondrial signal peptide) was generously donated by Dr. Abdussalam Azem from Tel Aviv University, Faculty of Life Sciences, Department of Biochemistry, Israel.

ABBREVIATIONS

MDH, malate dehydrogenase; Rho, rhodanese; IC_{50} - Inhibitory concentration for half-maximal signal in biochemical assay; EC_{50}, effective concentration for half-maximal signal in bacterial proliferation assays; CC_{50}, cytotoxicity concentration for half-maximal signal in human cell viability assays.

SUPPORTING INFORMATION

Supporting Information associated with this article can be found in the online version, which includes tabulation of all log(IC_{50}), log(EC_{50}), and log(CC_{50}) results with standard deviations; synthetic protocols and characterization data for test compounds (MS, ^{1}H-NMR, and HPLC purity); experimental protocols for protein synthesis and purification, and biochemical, bacterial proliferation, and human cell viability assays; and SMILES strings of compound structures.

REFERENCES

1. Centers for Disease Control and Prevention. *Antibiotic resistance threats in the United States, 2013*. Centers for Disease Control and Prevention: Atlanta, Georgia, USA, 2013; p 114.
2. Boucher, H. W.; Talbot, G. H.; Bradley, J. S.; Edwards, J. E.; Gilbert, D.; Rice, L. B.; Scheld, M.; Spellberg, B.; Bartlett, J. Bad bugs, no drugs: No ESKAPE! An update from the Infectious Diseases Society of America. *Clin. Infect. Dis.* **2009,** 48, 1-12.
3. Lewis, K. Platforms for antibiotic discovery. *Nat. Rev. Drug Discov.* **2013,** 12, 371-387.
4. Wright, G. D.; Sutherland, A. D. New strategies for combating multidrug-resistant bacteria. *Trends Mol. Med.* **2007,** 13, 260-267.
5. Bjarnsholt, T. The role of bacterial biofilms in chronic infections. *APMIS Suppl.* **2013**, 1-51.
6. Stewart, P. S.; Costerton, J. W. Antibiotic resistance of bacteria in biofilms. *Lancet* **2001,** 358, 135-138.
7. Singh, R.; Ray, P.; Das, A.; Sharma, M. Penetration of antibiotics through *Staphylococcus aureus* and *Staphylococcus epidermidis* biofilms. *J. Antimicrob. Chemother.* **2010,** 65, 1955-1958.
8. Hartl, F. U.; Bracher, A.; Hayer-Hartl, M. Molecular chaperones in protein folding and proteostasis. *Nature* **2011,** 475, 324-332.
9. Stefani, M.; Dobson, C. M. Protein aggregation and aggregate toxicity: new insights into protein folding, misfolding diseases and biological evolution. *J. Mol. Med. (Berl.)* **2003,** 81, 678-699.
10. Maisonneuve, E.; Ezraty, B.; Dukan, S. Protein aggregates: An aging factor involved in cell death. *J. Bacter.* **2008,** 190, 6070-6075.

11. Carmichael, J.; Chatellier, J.; Woolfson, A.; Milstein, C.; Fersht, A. R.; Rubinsztein, D. C. Bacterial and yeast chaperones reduce both aggregate formation and cell death in mammalian cell models of Huntington's disease. *Proc. Natl. Acad. Sci. U.S.A.* **2000,** 97, 9701-9705.

12. Bao, Y. P.; Cook, L. J.; O'Donovan, D.; Uyama, E.; Rubinsztein, D. C. Mammalian, yeast, bacterial, and chemical chaperones reduce aggregate formation and death in a cell model of oculopharyngeal muscular dystrophy. *J. Biol. Chem.* **2002,** 277, 12263-12269.

13. Park, H. K.; Lee, J. E.; Lim, J.; Jo, D. E.; Park, S. A.; Suh, P. G.; Kang, B. H. Combination treatment with doxorubicin and gamitrinib synergistically augments anticancer activity through enhanced activation of Bim. *BMC Cancer* **2014,** 14, 431.

14. Whitesell, L.; Lin, N. U. HSP90 as a platform for the assembly of more effective cancer chemotherapy. *Biochim. Biophys. Acta Mol. Cell Res.* **2012,** 1823, 756-766.

15. Whitesell, L.; Lindquist, S. L. HSP90 and the chaperoning of cancer. *Nat. Rev. Cancer* **2005,** 5, 761-772.

16. Chiappori, F.; Fumian, M.; Milanesi, L.; Merelli, I. DnaK as antibiotic target: Hot spot residues analysis for differential inhibition of the bacterial protein in comparison with the human HSP70. *PLoS One* **2015,** 10, e0124563.

17. Arita-Morioka, K.; Yamanaka, K.; Mizunoe, Y.; Ogura, T.; Sugimoto, S. Novel strategy for biofilm inhibition by using small molecules targeting molecular chaperone DnaK. *Antimicrob. Agents Chemother.* **2015,** 59, 633-641.

18. Sass, P.; Josten, M.; Famulla, K.; Schiffer, G.; Sahl, H. G.; Hamoen, L.; Brotz-Oesterhelt, H. Antibiotic acyldepsipeptides activate ClpP peptidase to degrade the cell division protein FtsZ. *Proc. Natl. Acad. Sci. U.S.A.* **2011,** 108, 17474-17479.

19. Evans, C. G.; Chang, L.; Gestwicki, J. E. Heat shock protein 70 (hsp70) as an emerging drug target. *J. Med. Chem.* **2010,** 53, 4585-4602.

20. Piper, P. W.; Millson, S. H. Spotlight on the microbes that produce heat shock protein 90-targeting antibiotics. *Open Biology* **2012,** 2, 120138.

21. Braig, K.; Otwinowski, Z.; Hegde, R.; Boisvert, D. C.; Joachimiak, A.; Horwich, A. L.; Sigler, P. B. The crystal structure of the bacterial chaperonin GroEL at 2.8 A. *Nature* **1994,** 371, 578-586.

22. Sigler, P. B.; Xu, Z.; Rye, H. S.; Burston, S. G.; Fenton, W. A.; Horwich, A. L. Structure and function in GroEL-mediated protein folding. *Annu. Rev. Biochem.* **1998,** 67, 581-608.

23. Horwich, A. L.; Farr, G. W.; Fenton, W. A. GroEL-GroES-mediated protein folding. *Chem. Rev.* **2006,** 106, 1917-1930.

24. Fenton, W. A.; Kashi, Y.; Furtak, K.; Horwich, A. L. Residues in chaperonin GroEL required for polypeptide binding and release. *Nature* **1994,** 371, 614-619.

25. Fenton, W. A.; Horwich, A. L. GroEL-mediated protein folding. *Protein Sci.* **1997,** 6, 743-760.

26. Horwich, A. L.; Fenton, W. A.; Chapman, E.; Farr, G. W. Two families of chaperonin: physiology and mechanism. *Annu. Rev. Cell. Dev. Biol.* **2007,** 23, 115-145.

27. Saibil, H. R.; Fenton, W. A.; Clare, D. K.; Horwich, A. L. Structure and allostery of the chaperonin GroEL. *J. Mol. Biol.* **2013,** 425, 1476-1487.

28. Chapman, E.; Farr, G. W.; Usaite, R.; Furtak, K.; Fenton, W. A.; Chaudhuri, T. K.; Hondorp, E. R.; Matthews, R. G.; Wolf, S. G.; Yates, J. R.; Pypaert, M.; Horwich, A. L. Global aggregation of newly translated proteins in an *Escherichia coli* strain deficient of the chaperonin GroEL. *Proc. Natl. Acad. Sci. U.S.A.* **2006,** 103, 15800-15805.

29. Fayet, O.; Ziegelhoffer, T.; Georgopoulos, C. The groES and groEL heat shock gene products of Escherichia coli are essential for bacterial growth at all temperatures. *J. Bacteriol.* **1989,** 171, 1379-1385.

30. Johnson, S. M.; Sharif, O.; Mak, P. A.; Wang, H. T.; Engels, I. H.; Brinker, A.; Schultz, P. G.; Horwich, A. L.; Chapman, E. A biochemical screen for GroEL/GroES inhibitors. *Bioorg. Med. Chem. Lett.* **2014,** 24, 786-789.

31. Abdeen, S.; Salim, N.; Mammadova, N.; Summers, C. M.; Frankson, R.; Ambrose, A. J.; Anderson, G. G.; Schultz, P. G.; Horwich, A. L.; Chapman, E.; Johnson, S. M. GroEL/ES inhibitors as potential antibiotics. *Bioorg. Med. Chem. Lett.* **2016,** 26, 3127-3134.

32. Safonova, T. V.; Fedyanina, L. V.; Trusov, S. N.; Feoktistova, T. S.; Sevbo, D. P.; Mikhailitsyn, F. S. Antitrichocephalous activity of the agents G-1730 and G-1732. *Meditsinskaya Parazitologiya i Parazitarnye Bolezni* **2003**, 21-22.

33. Stromberg, B. E.; Schlotthauer, J. C.; Conboy, G. A. The efficacy of closantel against Fascioloides magna in sheep. *J. Parasitol.* **1984,** 70, 446-447.

34. Cheng, T. J.; Wu, Y. T.; Yang, S. T.; Lo, K. H.; Chen, S. K.; Chen, Y. H.; Huang, W. I.; Yuan, C. H.; Guo, C. W.; Huang, L. Y.; Chen, K. T.; Shih, H. W.; Cheng, Y. S.; Cheng, W. C.; Wong, C. H. High-throughput identification of antibacterials against methicillin-resistant Staphylococcus aureus (MRSA) and the transglycosylase. *Bioorg. Med. Chem.* **2010,** 18, 8512-8529.

35. Johnson, S. M.; Connelly, S.; Wilson, I. A.; Kelly, J. W. Toward optimization of the linker substructure common to transthyretin amyloidogenesis inhibitors using biochemical and structural studies. *J. Med. Chem.* **2008,** 51, 6348-6358.

36. Connelly, S.; Mortenson, D. E.; Choi, S.; Wilson, I. A.; Powers, E. T.; Kelly, J. W.; Johnson, S. M. Semi-quantitative models for identifying potent and selective transthyretin amyloidogenesis inhibitors. *Bioorg. Med. Chem. Lett.* **2017,** 27, 3441-3449.

37. Johnson, S. M.; Connelly, S.; Wilson, I. A.; Kelly, J. W. Toward optimization of the second aryl substructure common to transthyretin amyloidogenesis inhibitors using biochemical and structural studies. *J. Med. Chem.* **2009,** 52, 1115-1125.

38. Abdeen, S.; Kunkle, T.; Salim, N.; Ray, A. M.; Mammadova, N.; Summers, C.; Stevens, M.; Ambrose, A. J.; Park, Y.; Schultz, P. G.; Horwich, A. L.; Hoang, Q. Q.; Chapman, E.; Johnson, S. M. Sulfonamido-2-arylbenzoxazole GroEL/ES Inhibitors as Potent Antibacterials against Methicillin-Resistant Staphylococcus aureus (MRSA). *J Med Chem* **2018,** 61, 7345-7357.

39. Heinz, L. J.; Panetta, J. A.; Phillips, M. L.; Reel, J. K.; Shadle, J. K.; Simon, R. L.; Whitesitt, C. A. Preparation of (Hetero)arylthioureas and Analogs as Amyloid β-protein Biosynthesis Inhibitors. US 5814646, 1998.

40. Abdeen, S.; Salim, N.; Mammadova, N.; Summers, C. M.; Goldsmith-Pestana, K.; McMahon-Pratt, D.; Schultz, P. G.; Horwich, A. L.; Chapman, E.; Johnson, S. M. Targeting the HSP60/10 chaperonin systems of *Trypanosoma brucei* as a strategy for treating African sleeping sickness. *Bioorg. Med. Chem. Lett.* **2016,** 26, 5247-5253.

41. Martin, R. J. Modes of action of anthelmintic drugs. *Vet. J.* **1997,** 154, 11-34.

42. Martin, R. J.; Robertson, A. P.; Bjorn, H. Target sites of anthelmintics. *Parasitology* **1997,** 114, S111-S124.

43. Kim, S.; Lieberman, T. D.; Kishony, R. Alternating antibiotic treatments constrain evolutionary paths to multidrug resistance. *Proc. Natl. Acad. Sci. U.S.A.* **2014,** 111, 14494-14499.

44. Parnas, A.; Nadler, M.; Nisemblat, S.; Horovitz, A.; Mandel, H.; Azem, A. The MitCHAP-60 disease is due to entropic destabilization of the human mitochondrial Hsp60 oligomer. *J. Biol. Chem.* **2009,** 284, 28198-28203.

45. Fleeman, R.; LaVoi, T. M.; Santos, R. G.; Morales, A.; Nefzi, A.; Welmaker, G. S.; Medina-Franco, J. L.; Giulianotti, M. A.; Houghten, R. A.; Shaw, L. N. Combinatorial libraries as a tool for the discovery of novel, broad-spectrum antibacterial agents targeting the ESKAPE pathogens. *J. Med. Chem.* **2015,** 58, 3340-3355.

46. Kwasny, S. M.; Opperman, T. J. Static biofilm cultures of Gram-positive pathogens grown in a microtiter format used for anti-biofilm drug discovery. *Curr. Protoc. Pharmacol.* **2010,** Chapter 13, Unit 13A 18.

SCHEMES, TABLES, & FIGURES

Scheme 1[a]

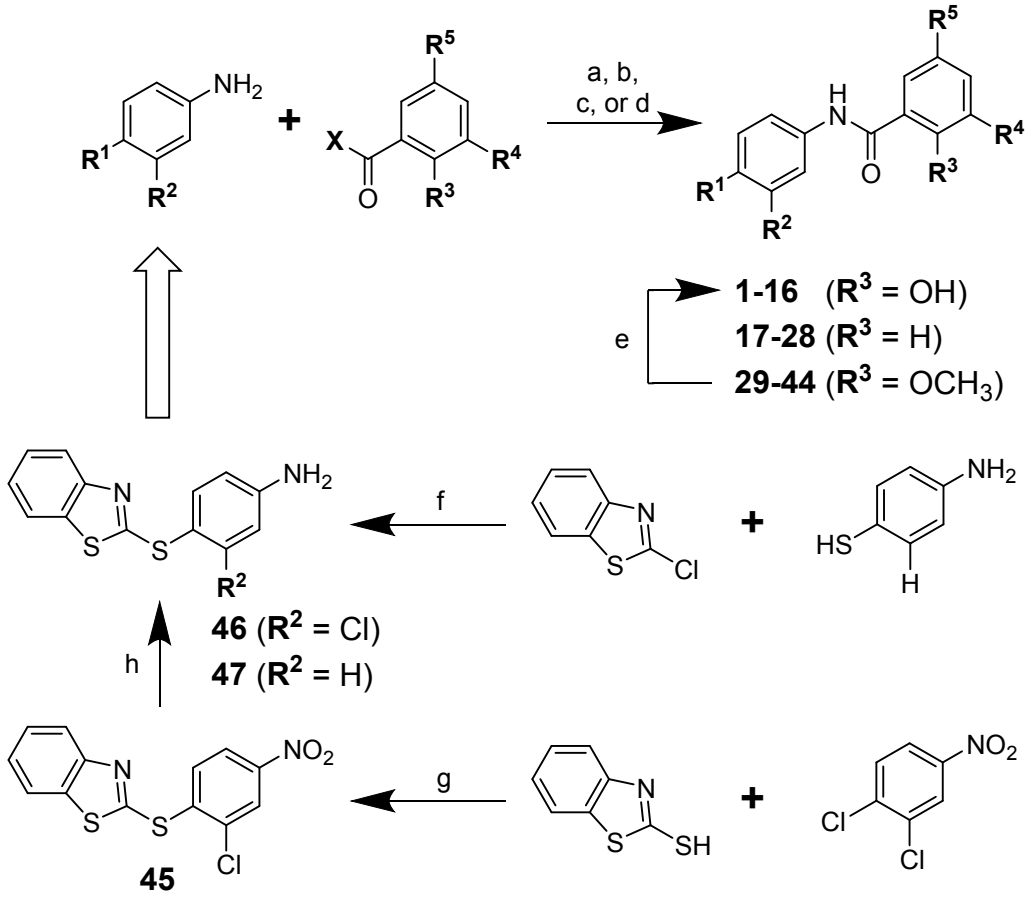

[a] Reagents and conditions: a) **X** = Cl: pyridine, CH_2Cl_2; b) **X** = OH: $SOCl_2$, 60°C, 1 h, then concentrate and add arylamine, pyridine, and CH_2Cl_2; c) **X** = OH: DCC, DMAP, CH_2Cl_2, 1 h, then add arylamine and pyridine; d) **X** = OH: EDC, HOBt•H_2O, TEA, CH_2Cl_2; e) BBr_3, DCM; f) K_2CO_3, EtOH; g) K_2CO_3, DMF, R.T.-80°C; h) Tin powder, 10% HCl/AcOH.

Table 1. Compilation of IC_{50} results for compounds tested in the GroEL/ES-mediated dMDH and dRho refolding assays, and the native MDH and Rho reporter counter-screens.

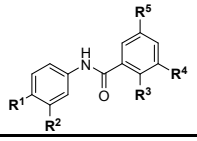

Compound Substituents & Substructures					Compound # / Name	Biochemical Assay IC_{50} (μM)			
R^1	R^2	R^3	R^4	R^5		Native Rho Reporter	Native MDH Reporter	GroEL/ES-dRho Refolding	GroEL/ES-dMDH Refolding
					Closantel	>100	6.1	1.5	2.2
					Rafoxanide	>100	25	2.2	4.3
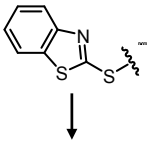	Cl	OH	Br	Br	**1**	>100	6.8	1.5	1.7
	Cl	OH	Br	H	**2**	>100	>63	3.8	9.5
	Cl	OH	H	Br	**3**	>100	>63	11	37
	Cl	OH	H	H	**4**	>100	>63	63	42
	H	OH	Br	Br	**5**	>100	8.4	1.3	2.7
	H	OH	Br	H	**6**	>100	>63	14	33
	H	OH	H	Br	**7**	>100	>63	30	38
	H	OH	H	H	**8**	>100	>63	87	40
H	Cl	OH	Br	Br	**9**	>100	27	47	24
H	Cl	OH	Br	H	**10**	>100	>63	>100	>100
H	Cl	OH	H	Br	**11**	>100	>63	>100	>100
H	Cl	OH	H	H	**12**	>100	>63	>100	>100
H	H	OH	Br	Br	**13**	>100	51	>100	61
H	H	OH	Br	H	**14**	>100	>63	>100	>100
H	H	OH	H	Br	**15**	>100	>63	>100	>100
H	H	OH	H	H	**16**	>100	>63	>100	>100
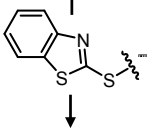	Cl	H	Br	Br	**17**	>100	>63	>100	>100
	Cl	H	Br (H)	H (Br)	**18**	>100	>63	>100	>100
	Cl	H	H	H	**19**	>100	>63	>100	>100
	H	H	Br	Br	**20**	>100	>63	>100	>100
	H	H	Br (H)	H (Br)	**21**	>100	>63	>100	>100
	H	H	H	H	**22**	>100	>63	>100	>100
H	Cl	H	Br	Br	**23**	>100	>63	>100	>100
H	Cl	H	Br (H)	H (Br)	**24**	>100	>63	>100	>100
H	Cl	H	H	H	**25**	>100	>63	>100	>100
H	H	H	Br	Br	**26**	>100	>63	>100	>100
H	H	H	Br (H)	H (Br)	**27**	>100	>63	>100	>100
H	H	H	H	H	**28**	>100	>63	>100	>100
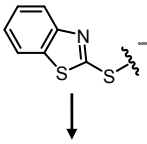	Cl	OCH_3	Br	Br	**29**	>100	>63	>100	>100
	Cl	OCH_3	Br	H	**30**	>100	>63	>100	>100
	Cl	OCH_3	H	Br	**31**	>100	>63	>100	>100
	Cl	OCH_3	H	H	**32**	>100	>63	>100	>100
	H	OCH_3	Br	Br	**33**	>100	>63	>100	>100
	H	OCH_3	Br	H	**34**	>100	>63	>100	>100
	H	OCH_3	H	Br	**35**	>100	>63	>100	>100
	H	OCH_3	H	H	**36**	>100	>63	>100	>100
H	Cl	OCH_3	Br	Br	**37**	>100	>63	>100	>100
H	Cl	OCH_3	Br	H	**38**	>100	>63	>100	>100
H	Cl	OCH_3	H	Br	**39**	>100	>63	>100	>100
H	Cl	OCH_3	H	H	**40**	>100	>63	>100	>100
H	H	OCH_3	Br	Br	**41**	>100	>63	>100	>100
H	H	OCH_3	Br	H	**42**	>100	>63	>100	>100
H	H	OCH_3	H	Br	**43**	>100	>63	>100	>100
H	H	OCH_3	H	H	**44**	>100	>63	>100	>100
					Vancomycin	>100	>63	>100	>100
					Daptomycin	>100	>63	>100	>100
					Ampicillin	>100	>63	>100	>100
					Rifampicin	>100	>63	>100	>100

Table 2. Compilation of EC_{50} results for compounds tested in the various bacterial proliferation assays.

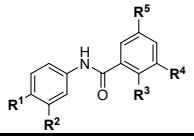

Compound Substituents & Substructures					Compound # / Name	Bacterial Proliferation EC_{50} (μM)						
						E. faecium	*S. aureus* Sensitive	*S. aureus* Resistant	*K. pneumoniae*	*A. baumannii*	*P. aeruginosa*	*E. cloacae*
					Closantel	1.2	0.47	0.47	>100	>100	>100	>100
R^1	R^2	R^3	R^4	R^5	**Rafoxanide**	0.99	0.32	0.34	>100	31	>100	40
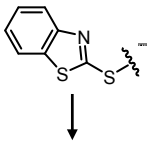	Cl	OH	Br	Br	**1**	0.52	0.36	0.55	>100	66	>100	>100
	Cl	OH	Br	H	**2**	24	0.45	0.71	>100	2.9	>100	>100
	Cl	OH	H	Br	**3**	15	0.12	0.17	>100	>100	>100	>100
	Cl	OH	H	H	**4**	64	0.31	0.45	>100	>100	>100	>100
	H	OH	Br	Br	**5**	0.88	0.44	0.52	>100	>100	>100	>100
	H	OH	Br	H	**6**	11	0.76	1.1	>100	12	>100	>100
	H	OH	H	Br	**7**	19	0.12	0.14	>100	>100	>100	>100
	H	OH	H	H	**8**	67	0.20	0.41	>100	>100	>100	>100
H	Cl	OH	Br	Br	**9**	73	0.66	1.1	95	46	>100	78
H	Cl	OH	Br	H	**10**	>100	1.3	2.0	>100	>100	>100	>100
H	Cl	OH	H	Br	**11**	>100	0.46	0.53	>100	>100	>100	>100
H	Cl	OH	H	H	**12**	>100	3.1	4.2	>100	>100	>100	>100
H	H	OH	Br	Br	**13**	>100	1.2	2.0	>100	>100	>100	>100
H	H	OH	Br	H	**14**	>100	6.4	10	>100	>100	>100	>100
H	H	OH	H	Br	**15**	>100	2.8	4.1	78	>100	>100	>100
H	H	OH	H	H	**16**	>100	28	51	>100	>100	>100	>100
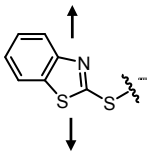	Cl	H	Br	Br	**17**	>100	>100	>100	>100	>100	>100	>100
	Cl	H	Br (H)	H (Br)	**18**	>100	>100	>100	>100	>100	>100	>100
	Cl	H	H	H	**19**	>100	43	>100	>100	>100	>100	>100
	H	H	Br	Br	**20**	>100	>100	>100	>100	>100	>100	>100
	H	H	Br (H)	H (Br)	**21**	>100	>100	>100	>100	>100	>100	>100
	H	H	H	H	**22**	>100	>100	>100	>100	>100	>100	>100
H	Cl	H	Br	Br	**23**	>100	14	12	>100	>100	>100	>100
H	Cl	H	Br (H)	H (Br)	**24**	>100	47	68	>100	>100	>100	>100
H	Cl	H	H	H	**25**	>100	>100	>100	>100	>100	>100	>100
H	H	H	Br	Br	**26**	>100	>100	>100	>100	>100	>100	>100
H	H	H	Br (H)	H (Br)	**27**	>100	>100	>100	>100	>100	>100	>100
H	H	H	H	H	**28**	>100	>100	>100	>100	>100	>100	>100
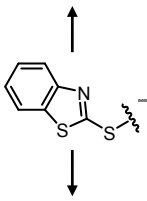	Cl	OCH_3	Br	Br	**29**	>100	>100	>100	>100	>100	>100	>100
	Cl	OCH_3	Br	H	**30**	>100	>100	>100	>100	>100	>100	>100
	Cl	OCH_3	H	Br	**31**	>100	>100	>100	>100	>100	>100	>100
	Cl	OCH_3	H	H	**32**	>100	>100	>100	>100	>100	>100	>100
	H	OCH_3	Br	Br	**33**	>100	>100	>100	>100	>100	>100	>100
	H	OCH_3	Br	H	**34**	>100	>100	>100	>100	>100	>100	>100
	H	OCH_3	H	Br	**35**	>100	>100	>100	>100	>100	>100	>100
	H	OCH_3	H	H	**36**	>100	>100	>100	>100	>100	>100	>100
H	Cl	OCH_3	Br	Br	**37**	>100	46	>100	>100	>100	>100	>100
H	Cl	OCH_3	Br	H	**38**	>100	>100	>100	>100	>100	>100	>100
H	Cl	OCH_3	H	Br	**39**	>100	>100	>100	>100	>100	>100	>100
H	Cl	OCH_3	H	H	**40**	>100	>100	>100	>100	>100	>100	>100
H	H	OCH_3	Br	Br	**41**	>100	>100	>100	>100	>100	>100	>100
H	H	OCH_3	Br	H	**42**	>100	>100	>100	>100	>100	>100	>100
H	H	OCH_3	H	Br	**43**	>100	>100	>100	>100	>100	>100	>100
H	H	OCH_3	H	H	**44**	>100	>100	>100	>100	>100	>100	>100
					Vancomycin	0.60	0.67	0.52	>100	>100	>100	>100
					Daptomycin	9.2	0.68	1.0	>100	>100	>100	>100
					Ampicillin	6.9	0.19	>100	>100	>100	>100	>100
					Rifampicin	0.13	<0.05	0.23	11	1.3	7.8	8.8

Table 3. Compilation of IC_{50} and CC_{50} results for compounds tested in the human HSP60/10-dMDH refolding assay and the liver (THLE-3) and kidney (HEK 293) cell viability assays.

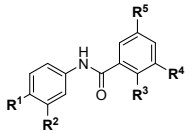

Compound Substituents & Substructures					Compound # / Name	HSP60/10-dMDH Refolding IC_{50} (μM)	Human Cell Viability CC_{50} (μM)	
R^1	R^2	R^3	R^4	R^5			Liver (THLE-3)	Kidney (HEK 293)
					Closantel	2.5	52	75
					Rafoxanide	2.8	24	>100
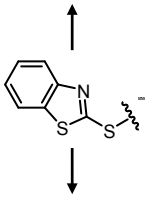	Cl	OH	Br	Br	**1**	4.2	14	76
	Cl	OH	Br	H	**2**	6.9	19	64
	Cl	OH	H	Br	**3**	>100	14	45
	Cl	OH	H	H	**4**	>100	34	64
	H	OH	Br	Br	**5**	4.7	20	66
	H	OH	Br	H	**6**	26	36	71
	H	OH	H	Br	**7**	>100	12	42
	H	OH	H	H	**8**	>100	33	74
H	Cl	OH	Br	Br	**9**	29	9.2	18
H	Cl	OH	Br	H	**10**	>100	16	32
H	Cl	OH	H	Br	**11**	>100	4.1	15
H	Cl	OH	H	H	**12**	>100	16	37
H	H	OH	Br	Br	**13**	63	25	34
H	H	OH	Br	H	**14**	>100	56	82
H	H	OH	H	Br	**15**	>100	16	35
H	H	OH	H	H	**16**	>100	68	>100
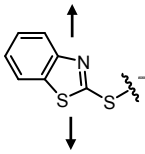	Cl	H	Br	Br	**17**	>100	>100	>100
	Cl	H	Br (H)	H (Br)	**18**	>100	88	>100
	Cl	H	H	H	**19**	>100	82	90
	H	H	Br	Br	**20**	>100	>100	>100
	H	H	Br (H)	H (Br)	**21**	>100	82	74
	H	H	H	H	**22**	>100	>100	>100
H	Cl	H	Br	Br	**23**	>100	45	53
H	Cl	H	Br (H)	H (Br)	**24**	>100	50	51
H	Cl	H	H	H	**25**	>100	>100	>100
H	H	H	Br	Br	**26**	>100	>100	>100
H	H	H	Br (H)	H (Br)	**27**	>100	>100	>100
H	H	H	H	H	**28**	>100	>100	>100
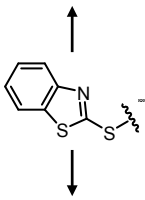	Cl	OCH_3	Br	Br	**29**	>100	>100	>100
	Cl	OCH_3	Br	H	**30**	>100	>100	>100
	Cl	OCH_3	H	Br	**31**	>100	>100	>100
	Cl	OCH_3	H	H	**32**	>100	>100	>100
	H	OCH_3	Br	Br	**33**	>100	>100	>100
	H	OCH_3	Br	H	**34**	>100	>100	>100
	H	OCH_3	H	Br	**35**	>100	>100	>100
	H	OCH_3	H	H	**36**	>100	>100	>100
H	Cl	OCH_3	Br	Br	**37**	>100	>100	>100
H	Cl	OCH_3	Br	H	**38**	>100	>100	>100
H	Cl	OCH_3	H	Br	**39**	>100	94	>100
H	Cl	OCH_3	H	H	**40**	>100	>100	>100
H	H	OCH_3	Br	Br	**41**	>100	>100	>100
H	H	OCH_3	Br	H	**42**	>100	>100	>100
H	H	OCH_3	H	Br	**43**	>100	>100	>100
H	H	OCH_3	H	H	**44**	>100	>100	>100
					Vancomycin	>100	>100	>100
					Daptomycin	>100	>100	>100
					Ampicillin	>100	>100	>100
					Rifampicin	>100	72	>100

Table 4. Compilation of EC_{50} values for inhibitors tested in the biofilm formation and penetration/bactericidal activity assays.

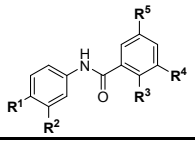

Compound Substituents & Substructures					Compound # / Name	*S. aureus* Proliferation & Biofilm Assay EC_{50} (μM)		
R^1	R^2	R^3	R^4	R^5		Planktonic Growth	Preventing Biofilm Formation	Killing Bacteria in Biofilms
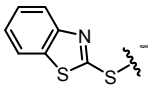	Cl	OH	Br	Br	**1**	0.36	0.72	2.4
	Cl	OH	Br	H	**2**	0.45	1.0	5.6
	H	OH	Br	Br	**5**	0.44	0.54	2.3
	H	OH	H	H	**8**	0.20	0.91	2.0
H	Cl	OH	H	Br	**11**	0.46	0.44	6.9
					Vancomycin	0.67	0.54	>100

Figure 1. A. Chemical structure of the initial GroEL/ES hit inhibitor, **1**, which was previously reported to potently inhibit the proliferation of *E. faecium* (EC_{50} = 0.15 μM) and *S. aureus* (EC_{50} = 0.20 μM).[31] Analogs of inhibitor **1** have been synthesized and evaluated in this study, where the $\mathbf{R^1}$ through $\mathbf{R^5}$ substituents and substructures have been systematically removed to probe for the contributions that each make to inhibiting chaperonin system biochemical functions and bacterial and human cell viabilities. **B.** Chemical structures of related compounds used as anthelmintics in veterinary medicine.

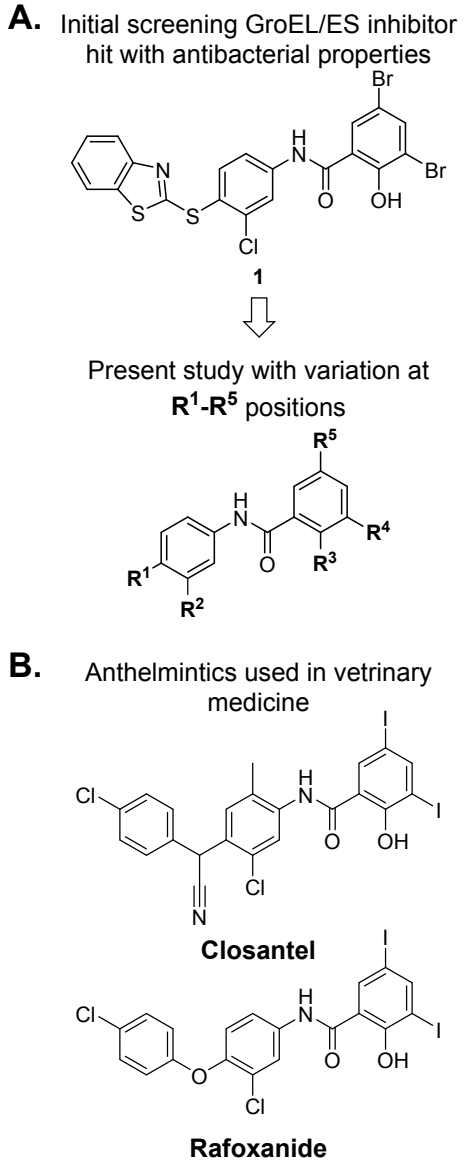

Figure 2. Correlation plots of IC_{50} values for compounds evaluated in the respective biochemical assays. **A.** Compounds inhibit nearly equipotently in the GroEL/ES-dMDH and the GroEL/ES-dRho refolding assays, supporting on-target effects (Spearman correlation coefficient comparing $\log(IC_{50})$ values in each assay is 0.9663, $p < 0.0001$). **B.** While some compounds inhibit in the native MDH enzymatic reporter counter screen, none inhibit native Rho enzymatic activity, further supporting on-target effects for inhibiting the chaperonin-mediated refolding cycle. Results plotted in the grey zones represent IC_{50} values higher than the maximum concentrations listed.

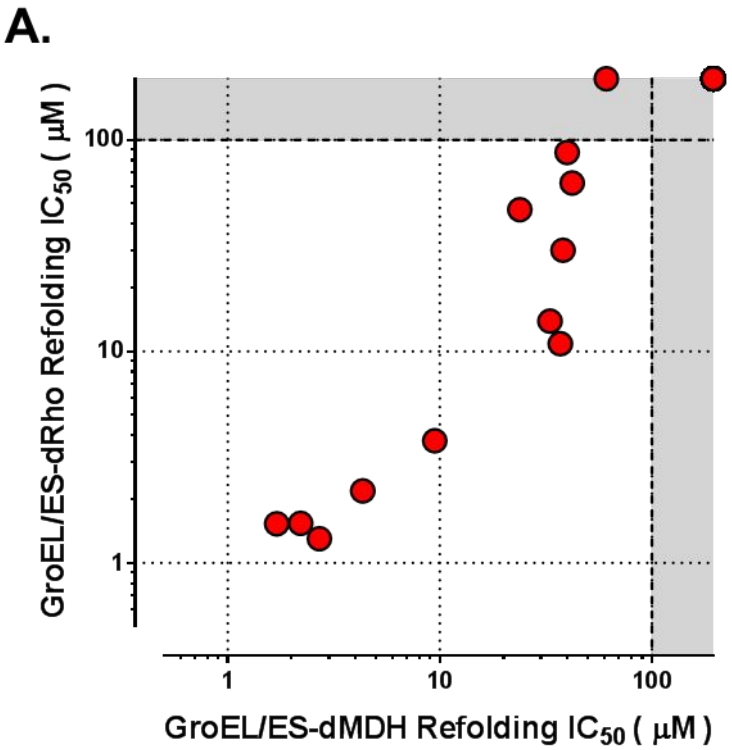

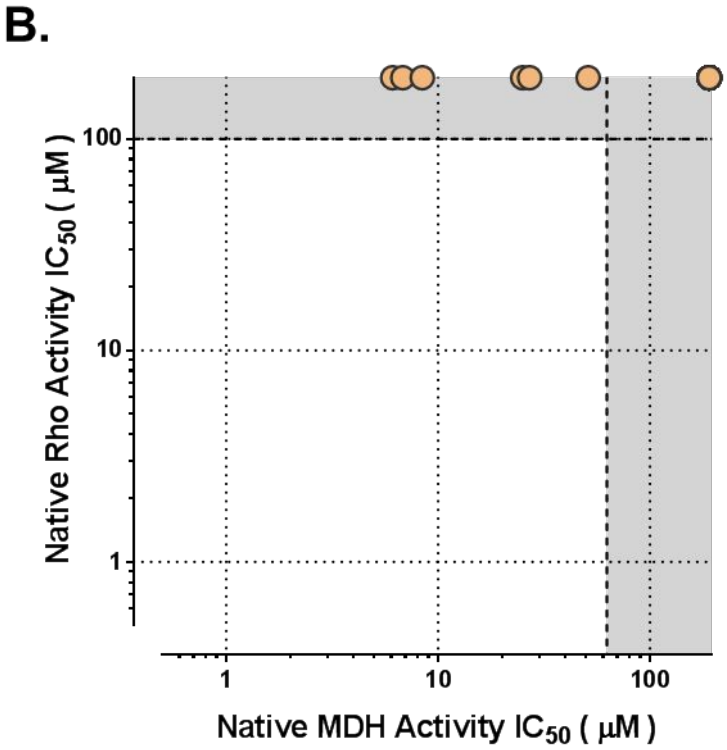
B.
Native Rho Activity IC50 (μM)
100
10
1
1
10
100
Native MDH Activity IC50 (μM)

Figure 3. Correlation plots comparing IC_{50} values for compounds tested in the GroEL/ES-dMDH refolding assay with EC_{50} values for inhibiting *E. faecium* (**A**) and MRSA (**B**) proliferation. While a general trend is observed between inhibiting the GroEL/ES chaperonin system and *E. faecium* proliferation (Spearman correlation coefficient comparing $\log(I/EC_{50})$ values in each assay is 0.9628, $p < 0.0001$), supporting on-target effects in bacteria, inhibitors are more potent against MRSA (Spearman correlation coefficient comparing $\log(I/EC_{50})$ values in each assay is 0.8042, $p < 0.0001$), suggesting potential off-target effects and/or greater GroEL/ES sensitivity in *S. aureus* bacteria. Results plotted in the grey zones represent IC_{50} and EC_{50} values higher than the maximum concentrations listed.

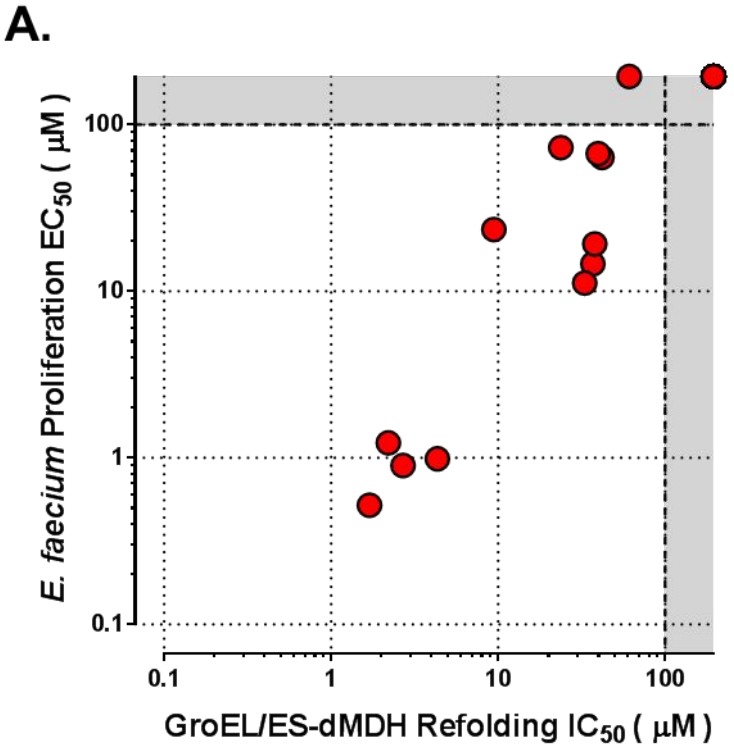

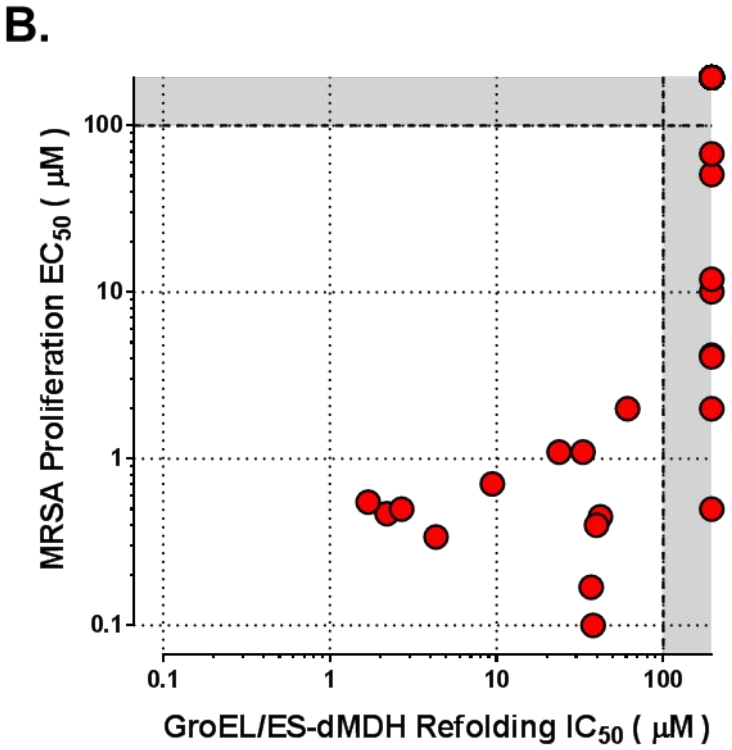
B.
MRSA Proliferation EC50 (μM)
100
10
1
0.1
0.1
1
10
100
GroEL/ES-dMDH Refolding IC50 (μM)

Figure 4. Correlation plots comparing human HSP60/10-dMDH and GroEL/ES-dMDH refolding assay IC_{50}, human cell viability CC_{50}, and MRSA proliferation EC_{50} results. **A.** Compounds inhibit the HSP60/10 and GroEL/ES chaperonin systems nearly equipotently, suggesting binding sites may be highly conserved between the two (Spearman correlation coefficient comparing log(IC_{50}) values in each assay is 0.8351, $p < 0.0001$). **B.** Despite compounds inhibiting human HSP60/10 *in vitro*, many exhibit low to no cytotoxic effects against human liver (THLE-3) and kidney (HEK 293) in cell viability assays (Spearman correlation coefficient values are 0.4791 ($p < 0.0008$) and 0.3286 ($p < 0.0258$) when comparing HSP60/10-dMDH refolding assay log(IC_{50}) values with liver and kidney cell viability log(CC_{50}) values, respectively). **C.** Lead analogs inhibit MRSA proliferation with high selectivity compared to cytotoxicity to human liver (THLE-3) and kidney (HEK 293) cells. Results plotted in the grey zones represent IC_{50}, CC_{50}, and EC_{50} values higher than the maximum concentrations listed.

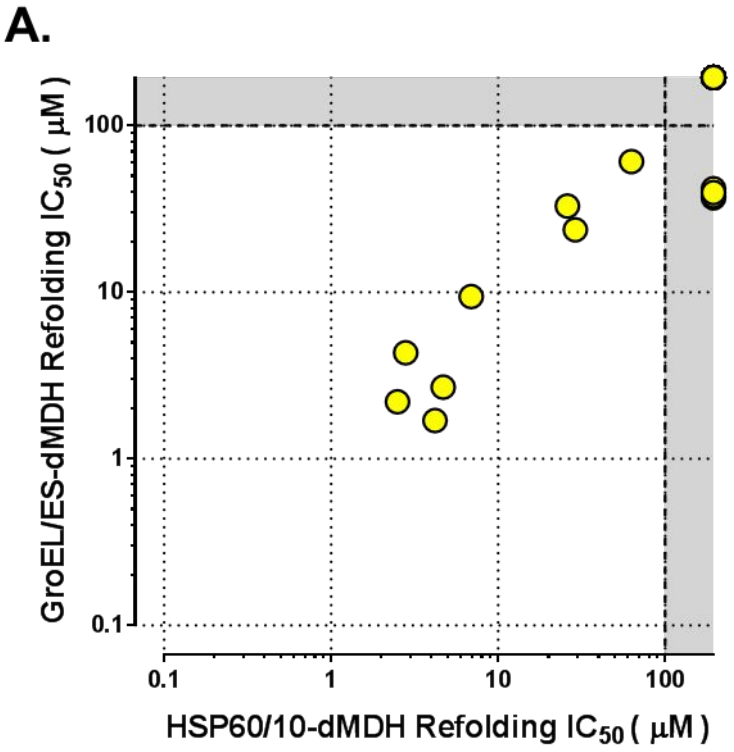

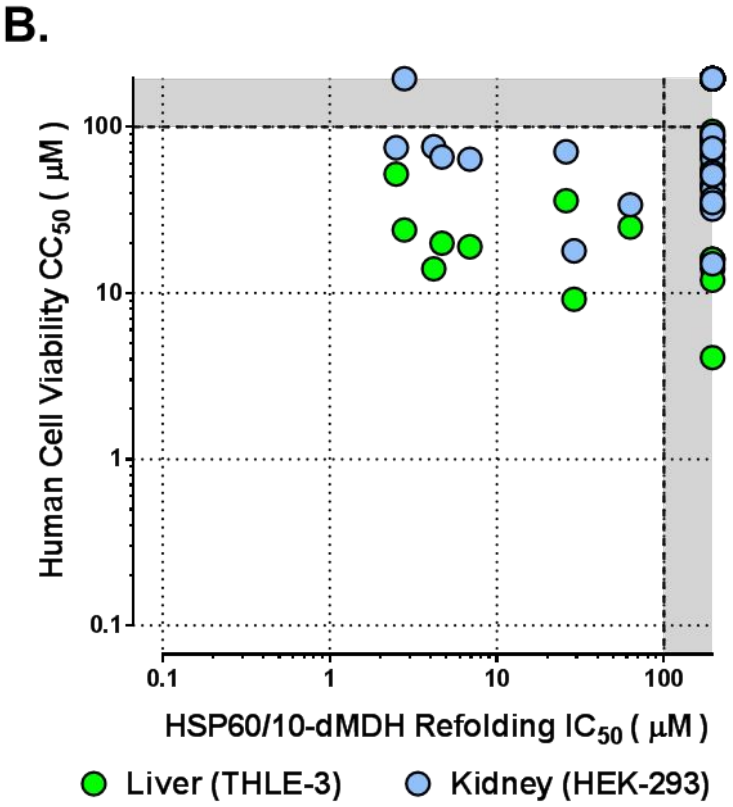
B.
Human Cell Viability CC50 (μM)
100
10
1
0.1
0.1
1
10
100
HSP60/10-dMDH Refolding IC50 (μM)
Liver (THLE-3)
Kidney (HEK-293)

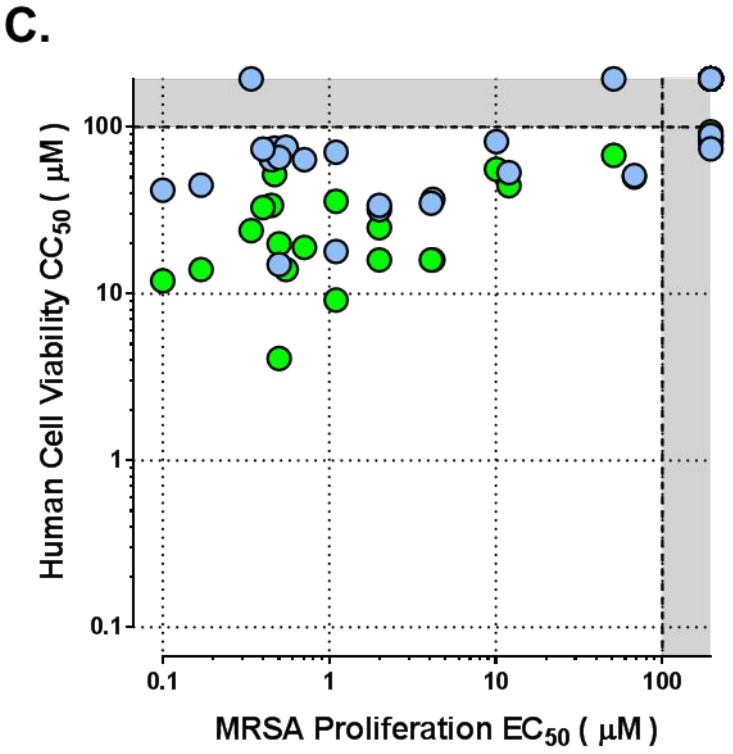
C.
Human Cell Viability CC50 (μM)
100
10
1
0.1
0.1
1
10
100
MRSA Proliferation EC50 (μM)

Figure 5. Exploring adaptive tolerance by MRSA bacteria to analogs **1**, **11**, vancomycin, and a previously-reported GroEL/ES inhibitor, "**28R**" (structure shown and numbering as previously reported).[38] Average EC_{50} values of compounds tested after each 24 h passage are plotted from triplicate analyses. MRSA rapidly evolved resistance to **28R**, but retained sensitivity to **1**, **11**, and vancomycin throughout 12 day experiment. Data plotted in the gray zones represent EC_{50} results beyond the assay detection limits (i.e., >100 μM).

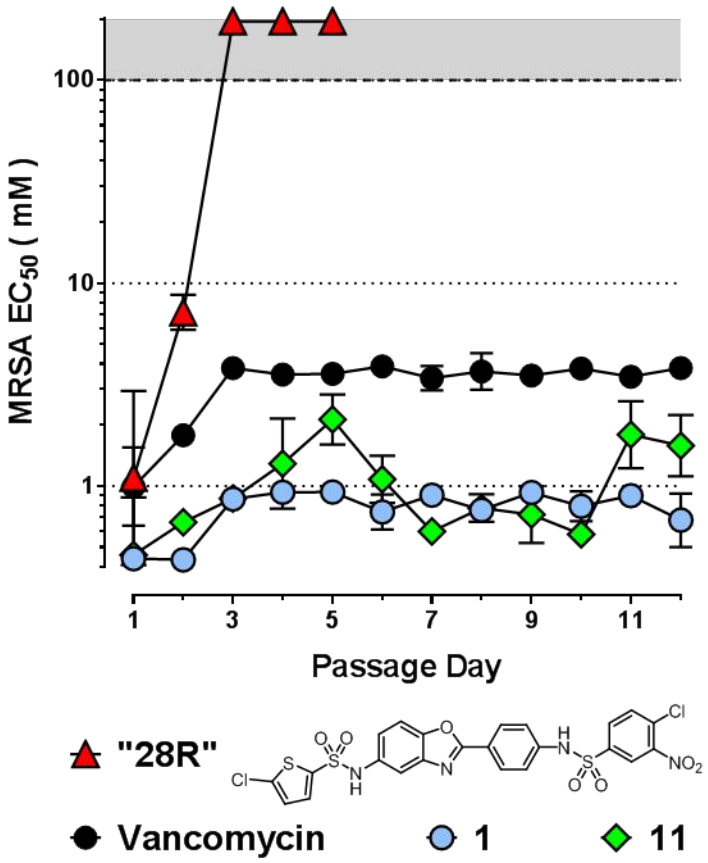

Figure 6. Representative dose-response plots for compound **1** (upper panel) and vancomycin (lower panel) evaluated in the *S. aureus* planktonic growth, biofilm formation, and biofilm penetration/bactericidal activity assays. Compound **1** is effective in all three assays, while vancomycin is ineffective at killing *S. aureus* bacteria in established biofilms. EC_{50} results for 1, vancomycin, and additional lead inhibitors tested in these assay are presented in **Table 4**.

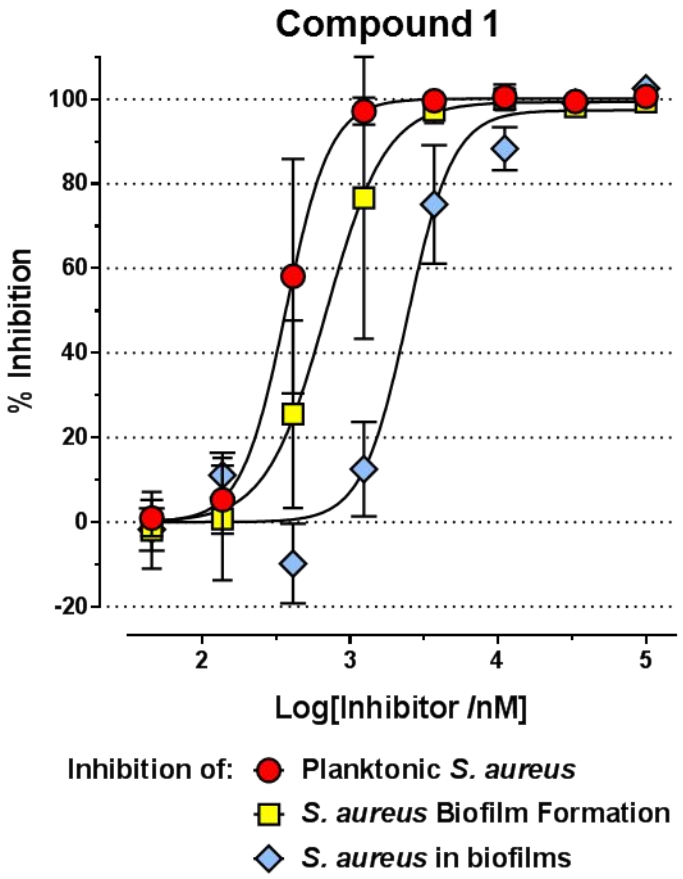

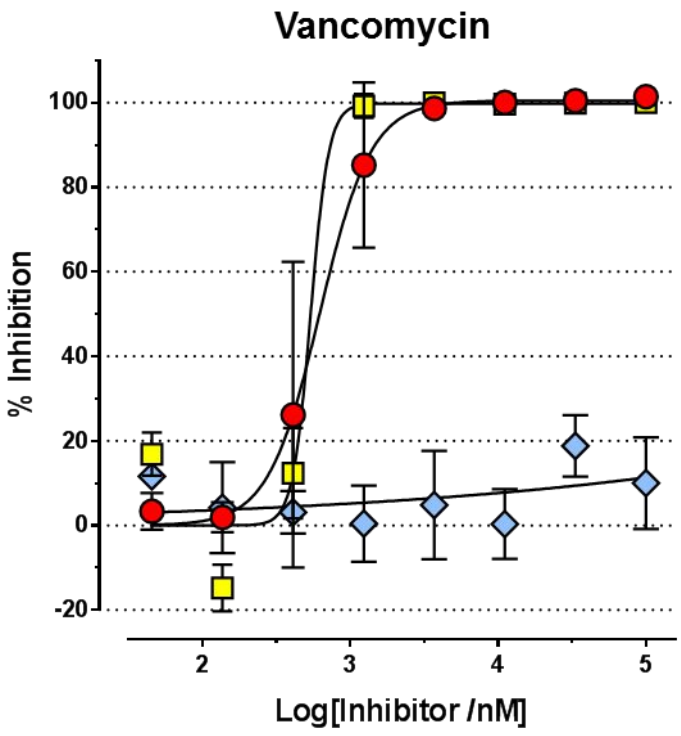
Vancomycin
% Inhibition
100
80
60
40
20
0
-20
2
3
4
5
Log[Inhibitor /nM]
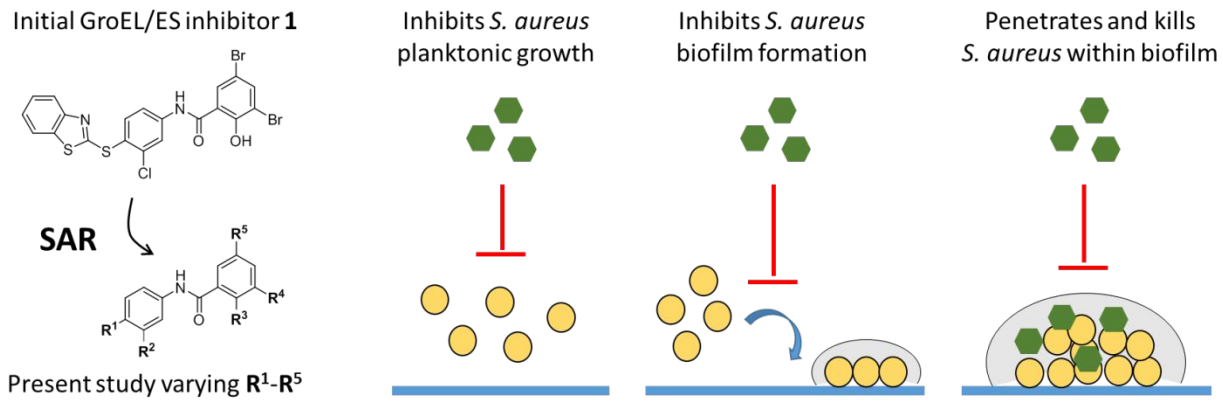
TABLE OF CONTENTS GRAPHIC